A QUANTITATIVE ACCOUNT OF THE ACTIVATION STEPS INVOLVED IN PHOTOTRANSDUCTION IN AMPHIBIAN PHOTORECEPTORS

By T. D. LAMB and E. N. PUGH Jr

From the Physiological Laboratory, University of Cambridge, Downing Street, Cambridge CB2 3EG, and the Psychology Department, University of Pennsylvania, 3815 Walnut Street, Philadelphia PA 19104–6196, USA

SUMMARY

1. We have undertaken a theoretical analysis of the steps contributing to the phototransduction cascade in vertebrate photoreceptors. We have explicitly considered only the activation steps, i.e. we have not dealt with the inactivation reactions.

2. From the theoretical analysis we conclude that a single photoisomerization leads to activation of the phosphodiesterase (PDE) with a time course which approximates a delayed ramp; the delay is contributed by several short first-order delay stages.

3. We derive a method for extracting the time course of PDE activation from the measured electrical response, and we apply this method to recordings of the photoresponse from salamander rods. The results confirm the prediction that the time course of PDE activation is a delayed ramp, with slope proportional to light intensity; the initial delay is about 10–20 ms.

4. We derive approximate analytical solutions for the electrical response of the photoreceptor to light, both for bright flashes (isotropic conditions) and for single photons (involving longitudinal diffusion of cyclic GMP in the outer segment). The response to a brief flash is predicted to follow a delayed Gaussian function of time, i.e. after an initial short delay the response should begin rising in proportion to t^2. Further, the response–intensity relation is predicted to obey an exponential saturation.

5. These predictions are compared with experiment, and it is shown that the rising phase of the flash response is accurately described over a very wide range of intensities. We conclude that the model provides a comprehensive description of the activation steps of phototransduction at a molecular level.

INTRODUCTION

The molecular basis of phototransduction has been studied intensively over the last decade. The steps involved in initiation of the response (i.e. in activation) are now well understood at a molecular level, but in contrast considerable doubt still surrounds the details of the mechanisms involved in termination of the state of activation (i.e. in inactivation). In this paper we show that there is now sufficient

quantitative information about each of the processes involved in *activation* to enable us to develop a formal quantitative description.

Our goal has been to provide a biophysical description of the *rising* phase of the photoresponse, applicable over an extremely wide range of intensities, from the level of single photoisomerizations upwards. To achieve this goal we have combined current knowledge of each of the molecular steps involved in initiating photo-transduction. Our model (or set of equations) is explicit in molecular terms, and depicts the activation steps in phototransduction as a series of relatively simple physical and biochemical processes, for which most of the parameters are basic physical quantities.

The concepts presented here represent a synthesis of ideas originating from many groups. We briefly summarize these ideas in the next section, but for a fuller treatment of the extensive literature on phototransduction we refer the reader to the reviews by Chabre (1985), Hofmann (1986), Pugh & Cobbs (1986), Stryer (1986), Liebman, Parker & Dratz (1987), Owen (1987), Yau & Baylor (1989), McNaughton (1990), Pugh & Lamb (1990) and in Hargrave, Hofmann & Kaupp (1992).

Our description of phototransduction differs from previous models in providing a quantitative description of each of the molecular steps involved in activation. In all theoretical treatments since the analysis of Baylor, Hodgkin & Lamb (1974), it has been *assumed* that a chain of reactions is involved in linking the absorption of a photon to the change in concentration of cytoplasmic messenger. Although Cobbs & Pugh (1987) and Forti, Menini, Rispoli & Torre (1989) treated the chain from physical principles, most previous models have not analysed the molecular details involved, but have instead described the chain in terms of an arbitrary mathematical function (e.g. Baylor *et al.* 1974; Sneyd & Tranchina, 1989). In contrast, the present model analyses the reactions of the cascade at a molecular level, taking account of diffusion both at the disc surface and in the cytoplasm.

BACKGROUND

In order to provide a background to the analysis that we are about to undertake, we now briefly review the protein reactions involved in the transduction cascade and also the electrophysiology of the rod outer segment.

Protein reactions of the transduction cascade

The biochemical reactions mediating the PDE cascade of transduction at the disc surface are indicated schematically in Fig. 1A. The three panels (Steps 1–3) represent activation respectively of rhodopsin (Rh*), of the G-protein (G_α*·GTP) and of the phosphodiesterase (PDE*).

Physical properties of the proteins

The concentration (density per unit area of disc membrane) and lateral diffusion coefficient of each of the three principal proteins of phototransduction are listed in Table 1, along with certain other parameter values and important symbol definitions.

Cytoplasmic reactions

Figure 1B summarizes the reactions occurring in the cytoplasm. The lower part represents the reactions of cyclic GMP: its synthesis, hydrolysis and binding to buffer
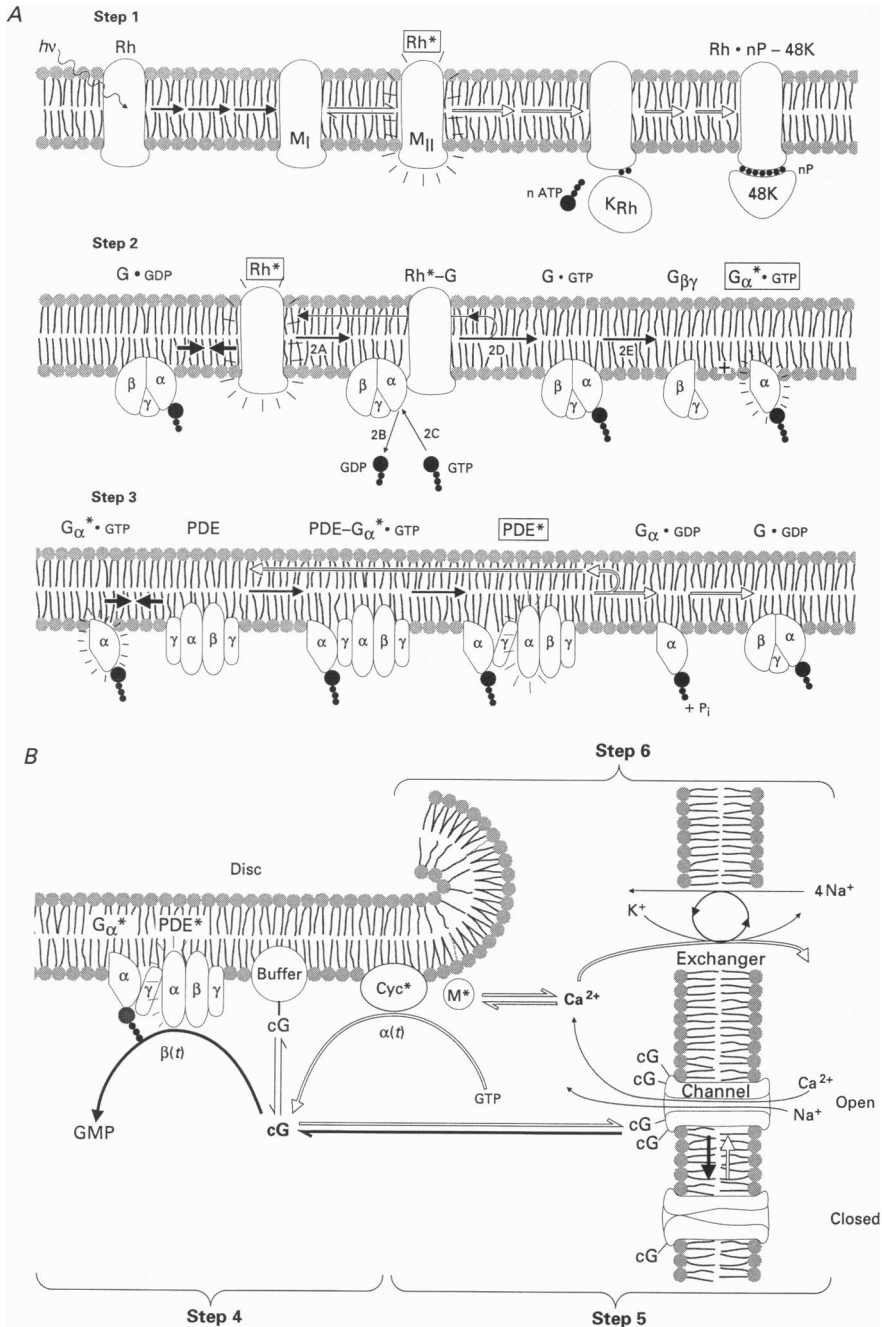
Fig. 1. Schematic of the reactions underlying phototransduction; for details see text and Pugh & Lamb (1990). Reactions mediating excitation are shown by filled arrows; reactions involved in recovery are shown by open arrows. *A*, protein reactions at the disc membrane; activated forms are in small boxes. Steps 1–3 show the reactions involving: rhodopsin (Rh*), the G-protein ($G_\alpha^*\cdot$GTP) and the phosphodiesterase (PDE*). *B*, cytoplasmic reactions of the diffusible messengers. Steps 4–6 show: the generation, buffering and hydrolysis of cyclic GMP (cG), channel activity and ion permeation, and calcium fluxes and action.

sites (Step 4), and its interaction with the ion channels in the plasma membrane (Step 5). The upper right hand section (Step 6) indicates the role of cytoplasmic calcium concentration, i.e. it shows the transmembrane Ca^{2+} fluxes and the hypothesized action of Ca_i^{2+} on guanylate cyclase via a modulatory protein; these reactions are considered only briefly in this paper.

TABLE 1. Important symbols of the model, and estimated parameter values for amphibian rods (see Appendix C)

Symbol	Value	Units	Definition
			Variables
Φ			Number of isomerizations at $t = 0$
$Rh^*(t)$, $G^*(t)$, $PDE^*(t)$			Number of activated rhodopsins, G-proteins, and PDE subunits
$cG(t)$		μM	Free concentration of cyclic GMP
$\beta(t)$, $\Delta\beta(t)$		s^{-1}	PDE hydrolytic rate constant, and its light-induced increment
$F(t)$, $R(t)$			Normalized current and response
			Protein concentrations and lateral diffusion coefficients
C_G	2500	μm^{-2}	Concentration (or area density) of G and PDE in disc membrane.
C_{PDE}	~ 167	μm^{-2}	
D_{Rh}	0·7	μm^2 s^{-1}	
D_G	~ 1·2	μm^2 s^{-1}	Lateral diffusion coefficients of Rh, $G_{\alpha\beta\gamma}$, G_α
$D_{G\alpha}$	~ 1·5	μm^2 s^{-1}	and PDE
D_{PDE}	~ 0·8	μm^2 s^{-1}	
			Other symbols
ν_{RG}, ν_{RP}		s^{-1}	Rate of activation of G* and PDE* per Rh*: eqns (A1)–(A2) and (A10)–(A15)
c_{GP}	~ 0·9		Coupling gain from G* to PDE*: eqns (3.2), (A8), (A14)
t_{eff}	~ 15	ms	Effective delay time: eqn (3.4)
β_{sub}	~ 6 × 10^{-6}	s^{-1}	Hydrolytic rate constant per PDE* subunit: eqn (4.4) or (C1)
n	2–3		Co-operativity of channel activation: eqn (5.1)
τ_ϕ		s	Characteristic time constant of transduction: eqn (6.9)
D_x	~ 7	μm^2 s^{-1}	Longitudinal diffusion coefficient of cyclic GMP in cytoplasm: eqns (4.5), (C4)

Electrophysiology

Families of electrical responses to brief flashes of increasing intensity exhibit a characteristic form of rising phase (see Fig. 7A). At early times the response is linear with intensity and has a power-law time dependence (Penn & Hagins, 1972; Baylor et al. 1974; Baylor, Lamb & Yau, 1979). Over a wide range of intensities the earliest phase of the response $r(t)$ to a brief flash (and the whole of the response to a dim flash) is well-described by

$$r(t) = k_1 I t^{N-1} e^{-t/\tau}, \tag{1}$$

where I is the light intensity and k_1 is a constant (in appropriate units). For rods at room temperature the exponent is $N-1 \approx 3$ and the time constant is $\tau \approx 200$–800 ms.

Although the linear intensity dependence of eqn (1) provides a good description of

the amplitude when the response is small, saturation sets in with larger responses. The form of the response–intensity relation at fixed times up to about 1 s has been shown to be fitted by the equation

$$R(t) = 1 - \exp[-I k_2(t)], \tag{2}$$

where $R(t)$ is the normalized response $r(t)/r_{max}$, and $k_2(t)$ is a constant at any particular time (Lamb, McNaughton & Yau, 1981). Possible bases for the form of this equation have been given by Baylor *et al.* (1974) and Lamb *et al.* (1981). Our analysis provides an alternative description to both these equations.

THEORY

In this section we present a theoretical analysis of the activation steps in the scheme outlined in Fig. 1. We ignore inactivation reactions, and we restrict consideration to intensities at which the protein reactions are linear with the number of photoisomerizations. It is possible to show that for the first 0·5 s of the response to flashes of up to *ca* 10^5 isomerizations these restrictions have little effect. For simplicity, we consider only the responses to brief flashes. We denote the *quantities* of the activated proteins by the italic forms $Rh^*(t)$, $G^*(t)$ and $PDE^*(t)$.

Step 1: Activation of rhodopsin

Equation for $Rh^*(t)$

It is now clear that the active form of rhodopsin, Rh*, can be identified with metarhodopsin II in a form prior to its phosphorylation by rhodopsin kinase and capping by the 48 kDa protein (reviewed in Chabre, 1985; Hofmann, 1986; see Fig. 1*A*). Spectrophotometric studies have shown that metarhodopsin II is formed very rapidly after photoisomerization. In amphibian rods at 22 °C the reaction has a time constant τ_R of 1·4 ms (rate constant 740 s^{-1}; Baumann, 1978). Hence, for a flash isomerizing Φ rhodopsin molecules at $t = 0$, the mean number $Rh^*(t)$ of activated rhodopsin molecules will be

$$Rh^*(t) = \Phi[1 - \exp(-t/\tau_R)]. \tag{1.1}$$

For the purposes of our subsequent analysis it is convenient to adopt the nomenclature step(t) and ramp(t) to denote the step and ramp functions, defined as zero for $t < 0$ and as unity and t respectively for $t > 0$. It is also helpful to employ the short-hand notation '* delay $(\tau_1, .. \tau_n, t)$' to denote convolution with n first-order delay stages having time constants $\tau_1, .. \tau_n$. With this terminology eqn (1.1) may be written as

$$Rh^*(t) = \Phi \, \text{step}(t) * \text{delay}(\tau_R, t). \tag{1.2}$$

Step 2: Activation of the G-protein by rhodopsin

*Biochemical mechanism of catalysis by Rh**

All the available evidence is consistent with the idea (put forward by Liebman & Pugh, 1979) that activation of the transduction cascade is brought about by the random lateral diffusion of Rh* and its target molecule, now established as the G-protein.

Upon contact between Rh* and a molecule of G-protein, a series of 'microsteps' is initiated, indicated schematically as Step 2 of Fig. 1A. This series of reactions leads ultimately to generation of the activated G* ($= G_\alpha^* \cdot GTP$) as well as to separation of the G-protein from Rh*, so that the single molecule of Rh* is able to undergo the cycle repetitively. The sequence of microsteps (in the forward direction) consists of the following:

2A: Rh* binds to $G \cdot GDP$, forming Rh*–$G \cdot GDP$,
2B: GDP is released, leaving Rh*–G (without nucleotide),
2C: GTP is bound, forming Rh*–$G \cdot GTP$,
2D: Rh* separates from $G \cdot GTP$,
2E: $G \cdot GTP$ separates into its subunits $G_\alpha^* \cdot GTP$ and $G_{\beta\gamma}$.

The evidence supporting this scheme has been reviewed by Kühn (1984), Chabre (1985), Hofmann (1986), Stryer (1986) and Hargrave *et al.* (1991).

Diffusional contact between Rh and the G-protein*

Before the series of microsteps 2A–2E can occur, the Rh* molecule must make contact with any one of the large number of inactive $G \cdot GDP$ molecules on the disc membrane. Since the GDP form of the holo-G-protein is almost exclusively membrane-bound, excitation cannot spread from Rh* to G-protein via the cytoplasm, and instead such contact must occur by means of mutual lateral diffusion of Rh* (which is an integral membrane protein) and the G-protein (which is a peripheral protein), within or at the surface of the disc membrane (see Liebman *et al.* 1987).

In Appendix A we consider such diffusional contact theoretically and we show that, whether or not the reaction proceeds at the diffusion limit, the rate ν_{RG} of activation of $G \cdot GTP$ by a single Rh* may (to a good approximation) be taken to be constant, over times from milliseconds to hundreds of milliseconds after isomerization.

Equation for the quantity of activated G-protein

Thus, in a region of outer segment exposed to Φ photoisomerizations at $t = 0$, the quantity of the activated form $G_\alpha^* \cdot GTP$ is (in the absence of inactivation reactions) given by eqn (A4) as

$$G^*(t) = \Phi \, \nu_{RG} \, \mathrm{ramp}(t) * \mathrm{delay}(\tau_R, \tau_{2C}, \tau_{2E}, t), \qquad (2.1)$$

where the dominant time constants of the series of microsteps are assumed to be τ_{2C} and τ_{2E}, associated with Steps 2C and 2E (p. 751).

In eqn (A2) of Appendix A we show that the diffusion limit on the rate ν_{RG} is given by

$$\nu_{RG} \lesssim 1{\cdot}5 \, (D_{Rh} + D_G) \, C_G, \qquad (2.2)$$

where D_{Rh} and $D_G \, (\mu\mathrm{m}^2 \, \mathrm{s}^{-1})$ represent the lateral diffusion coefficients of Rh* and $G \cdot GDP$, and where C_G (molecules $\mu\mathrm{m}^{-2}$) represents the concentration of $G \cdot GDP$ in the membrane. Our estimates of these parameters (see Table 1 and Appendix C) are $D_{Rh} + D_G \approx 1{\cdot}9 \, \mu\mathrm{m}^2 \, \mathrm{s}^{-1}$ and $C_G = 2500$ molecules $\mu\mathrm{m}^{-2}$, giving $\nu_{RG} \lesssim 7000$ G* s^{-1} per Rh*.

Step 3: Activation of PDE by $G_\alpha^* \cdot GTP$

Biochemical mechanism of activation of the PDE

The mechanisms believed to be involved in activation of the PDE are indicated schematically in Fig. 1, Step 3. The active subunit of the G-protein, $G_\alpha^* \cdot GTP$, binds stoichiometrically to a γ-subunit of the PDE, thereby removing an inhibitory constraint imposed by the γ-subunit. The earlier evidence in support of this mechanism of activation has been reviewed by Stryer (1986). More recent evidence has shown that the PDE in fact possesses two γ-subunits, and that the binding of two $G_\alpha^* \cdot GTP$'s is necessary for full activation; the binding of a single $G_\alpha^* \cdot GTP$ activates only a fraction of the total enzymatic activity (e.g. Deterre, Bigay, Forquet, Robert & Chabre, 1988; Whalen, Bitensky & Takemoto, 1990). Although there have been claims that the γ-subunit separates from the remainder of the PDE once the $G_\alpha^* \cdot GTP$ has bound to it, an alternative view supported by recent evidence is that such separation does not occur (e.g. Gray-Keller, Biernbaum & Bownds, 1990; Wensel & Stryer, 1990). Instead each γ-subunit may remain associated with the $PDE_{\alpha\beta}$, but with its inhibitory effect somehow relieved. In any event the actual physical disposition of the γ-subunit following the binding of $G_\alpha^* \cdot GTP$ does not affect the conclusions we draw concerning the time course of PDE activation.

Effect of two γ–subunits

There is some dispute about the extent of activation elicited by the binding of each $G_\alpha^* \cdot GTP$ to the PDE (Deterre *et al.* 1988; Whalen *et al.* 1990). However, it appears that the binding is very tight, and there is no convincing evidence that the $G_\alpha^* \cdot GTP$ separates from the γ-subunit of the PDE, even after extraction of the protein from the rod. In the case of tight binding it is possible to assume that on average half the $G_\alpha^* \cdot GTP$ is bound to each of the sites. Accordingly, the simplest way to take account of the effect of the two γ-subunits is to assume that the binding of each $G_\alpha^* \cdot GTP$ produces an effect corresponding to the average activity of the two sites. Thus it is most appropriate to define $PDE^*(t)$ as the quantity of activated PDE catalytic *subunits*, with each subunit having a hydrolytic activity half that of the fully activated multimer (i.e. $\frac{1}{2} k_{cat}/K_m$, see p. 727).

Diffusional contact between $G_\alpha^* \cdot GTP$ and PDE

Liebman *et al.* (1987) and Uhl, Wagner & Ryba (1990) have each summarized a number of properties of the activation of PDE by $G_\alpha^* \cdot GTP$ which lead them to conclude that contact between the proteins occurs not via cytoplasmic diffusion as proposed by Chabre (1985), but instead as a result of diffusion at the disc membrane surface, i.e. that $G_\alpha^* \cdot GTP$ does not move into the cytoplasm during the normal light response.

As a starting point we accept these arguments, and in Appendix A we investigate the extent of spatial spread of activated G-protein. We show that lateral diffusion at the disc surface occurs so rapidly that only a small proportion of $G_\alpha^* \cdot GTP$ remains within a region where its concentration exceeds the native concentration of activatable PDE subunits. This means that the PDE concentration is affected over a substantial area, so that depletion of the inactive PDE will not be particularly

localized to the point of photoisomerization. Thus the results in Appendix A indicate that lateral diffusion at the disc surface does *not* provide a significant limit to the rate of reaction between $G_\alpha^* \cdot GTP$ and PDE_γ, and they indicate that the reaction will proceed approximately according to the Law of Mass Action.

Solution for PDE*(t)

The analysis shows that the quantity of activated PDE* subunits may be expressed simply as a scaled (and slightly delayed) function of the quantity of $G_\alpha^* \cdot GTP$. Hence, from eqn (A 17), we obtain

$$PDE^*(t) = \Phi \, \nu_{RP} \, \text{ramp}(t) * \text{delay}(\tau_R, \tau_{2C}, \tau_{2E}, \tau_{P1}, \tau_{P2}, \tau_{P3}, t), \qquad (3.1)$$

where

$$\nu_{RP} = \nu_{RG} \, c_{GP} \qquad (3.2)$$

is the rate of activation of PDE* subunits by a single molecule of Rh*, and the parameter c_{GP} is referred to as the coupling gain for the activation of PDE by the G-protein. In Appendix A we show that, for the parameters of the amphibian rod outer segment, the diffusion limit on c_{GP} is quite close to unity, so that $\nu_{RP} \approx \nu_{RG}$.

The three additional delay stages represent the time τ_{P1} for first contact between a single $G_\alpha^* \cdot GTP$ and a PDE, the time constant τ_{P2} of the reaction of $G_\alpha^* \cdot GTP$ with PDE_γ, and the time constant τ_{P3} of removal of inhibition of the PDE once a $G_\alpha^* \cdot GTP$ has bound to a PDEγ. In Appendix A we show that the first contact time τ_{P1} should be given approximately by $\{3 (D_{G\alpha} + D_{PDE}) C_{PDE}\}^{-1}$, which yields a value of *ca* 1 ms; see eqn (A16). We assume that the latter two delays, τ_{P2} and τ_{P3}, are first-order, and that they are short.

The conclusion that diffusion at the surface of the disc membrane does not significantly hinder the rate of reaction has the implication that an aqueous path for diffusion would not appreciably increase the rate of reaction. Even if $G_\alpha^* \cdot GTP$ went into aqueous solution rapidly (and there is no evidence that it does so) and rapidly reached its target, the limiting value for the reaction rate could only increase by a small amount. So, although we cannot rule out the possibility of aqueous diffusion in this step, the analysis in Appendix A shows that there is no need to invoke such a mechanism, and that it would in any case not alter our equation for the activation of PDE.

Delayed ramp approximation

Equation (3.1) represents the 'output' of the PDE cascade of reactions in response to a brief flash of light, ignoring inactivation reactions and any competition for substrate which may occur at very high intensities. Since the six individual delay stages (τ_R, τ_{2C}, τ_{2E}, τ_{P1}, τ_{P2} and τ_{P3}), which together create a composite low-pass filtering effect, are each likely to be small with respect to the time-scale of our interest in the electrical response, it will be reasonable to approximate the term delay(...) in eqn (3.1) as a pure time delay. With this substitution eqn (3.1) reduces to the simple form of a 'delayed ramp'

$$PDE^*(t) \approx \Phi \, \nu_{RP} \, \text{ramp}(t - t_{eff}), \qquad (3.3)$$

where a limit on the effective delay time t_{eff} is given by

$$t_{eff} \lesssim \tau_R + \tau_{2C} + \tau_{2E} + \tau_{P1} + \tau_{P2} + \tau_{P3}. \qquad (3.4)$$

It must be stressed that eqn (3.3) is only an approximation, and that it is unlikely to be accurate at short times, i.e. it will be most accurate for $t \gg t_{\mathrm{eff}}$.

Of the six time constants in eqn (3.4), we have firm information about only two, the time constant of metarhodopsin II formation, $\tau_{\mathrm{R}} \approx 1 \cdot 5$ ms, and the time to first contact between a $\mathrm{G}_{\alpha}* \cdot \mathrm{GTP}$ and a PDE, $\tau_{\mathrm{P1}} \approx 1$ ms. For comparison, Cobbs & Pugh (1987), in their recordings of the earliest rising phase of the electrical response to very intense flashes ($\Phi > 10^8$), observed an irreducible total delay of about 7 ms before the onset of the response, which they described in terms of four first-order stages with time constants of about 2 ms.

Form of the solutions for the protein reactions

The solutions for the photon-induced change in quantity of the activated proteins Rh*, $\mathrm{G}_{\alpha}* \cdot \mathrm{GTP}$ and PDE*, given by eqns (1.2), (2.1) and (3.1) or (3.3), are illustrated in Fig. 2.
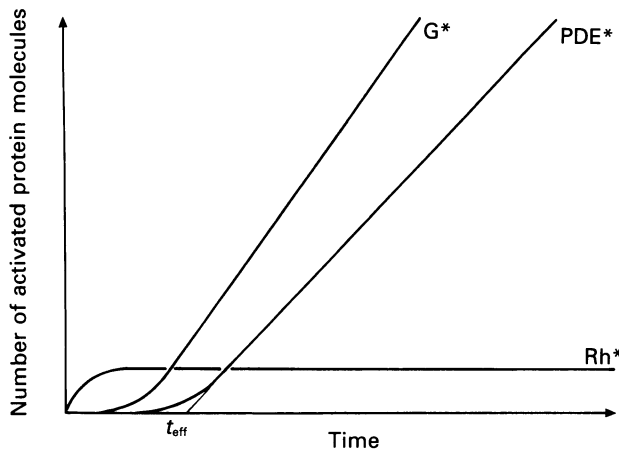

Fig. 2. Predicted time course for the activated forms of rhodopsin, G-protein and PDE in response to Φ photoisomerizations. The curves represent the concentrations $Rh*(t)$, $G*(t)$ and $PDE*(t)$ predicted by eqns (1.2), (2.1), (3.1) and (3.3). After an initial delay: $Rh*(t)$ approximates a steady value of Φ, $G*(t)$ rises with a slope of $\Phi \nu_{\mathrm{RG}}$, and $PDE*(t)$ rises with a slightly smaller slope of $\Phi \nu_{\mathrm{RP}}$; $PDE*(t)$ may be approximated as a ramp starting at t_{eff}.

Step 4: Cyclic GMP concentration

Hydrolytic activity induced by activation of PDE*

We shall denote the free cytoplasmic concentration of cyclic GMP as $cG(x,t)$, abbreviated simply as cG. Since the resting dark concentration of approximately $4 \,\mu\mathrm{M}$ (see below) is much smaller than the Michaelis constant K_{m} of the hydrolytic site on the PDE ($K_{\mathrm{m}} \geqslant 40 \,\mu\mathrm{M}$), the rate of hydrolysis of cyclic GMP by the activated PDE will proceed as a first-order reaction, with

$$\text{Rate of hydrolysis} = PDE*(t) \left[\tfrac{1}{2} k_{\mathrm{cat}}/K_{\mathrm{m}}\right] cG, \qquad (4.1)$$

(in units of molecules of cyclic GMP s^{-1}). The term in square brackets represents the

hydrolytic activity per activated subunit of enzyme ($s^{-1} \mu M^{-1}$), where k_{cat} (s^{-1}) is the hydrolytic velocity of the fully-activated PDE* (i.e. per mole of the holo-enzyme) at a saturating concentration of cyclic GMP. Note that this terminology refers the rate of hydrolysis to the number of activated *subunits*, rather than *molecules*, of PDE (see p. 725).

The rate of hydrolysis in the isotropic case of eqn (4.1) may be converted to a rate of change of total cyclic GMP concentration (averaged over the whole outer segment) by dividing by the cytoplasmic volume V_{cyto} and Avogadro's number N_{Av}. This value may in turn be converted to the rate of change of free cyclic GMP concentration by further dividing by the buffering power BP of the cytoplasm for cyclic GMP; in Appendix C we conclude that the buffering power is relatively small, with $BP \approx 2$. Hence the hydrolysis by PDE in eqn (4.1) corresponds to a rate of change of cG, averaged over the outer segment, of

$$\mathrm{d}cG/\mathrm{d}t = -\left[\frac{PDE^*(t)\,\tfrac{1}{2}k_{cat}/K_m}{V_{cyto}\,N_{Av}\,BP}\right]cG. \qquad (4.2)$$

Photon-induced increase in activity

The term in square brackets in eqn (4.2) represents $\Delta\beta(t)$, the light-induced increment in effective rate constant $\beta(t)$ of hydrolysis. (This definition of the rate constant $\beta(t)$ differs by the factor BP from that of Hodgkin & Nunn, 1988, in that it explicitly includes allowance for the buffering power for cyclic GMP). From eqn (4.2), $\Delta\beta(t)$ may be written as

$$\Delta\beta(t) = PDE^*(t)\,\beta_{sub}, \qquad (4.3)$$

where β_{sub}, defined as

$$\beta_{sub} = \frac{\tfrac{1}{2}k_{cat}/K_m}{V_{cyto}\,N_{Av}\,BP}, \qquad (4.4)$$

is the hydrolytic rate constant per activated subunit of PDE.

Differential equation for $cG(x,t)$

From the previous analyses of Lamb *et al.* (1981), Cobbs & Pugh (1987) and Hodgkin & Nunn (1988), the differential equation applicable to the generation, removal, binding and longitudinal diffusion of cyclic GMP can be written as the one-dimensional diffusion equation

$$\partial cG/\partial t = \alpha - \beta\,cG + D_x\,\partial^2 cG/\partial x^2. \qquad (4.5)$$

Here α is the effective cyclase rate and β is the effective PDE rate constant, and α, β and cG are each functions of longitudinal position x, as well as of t. D_x is the effective longitudinal diffusion coefficient for the movement of cyclic GMP in the outer segment cytoplasm; see Appendix C. In isotropic conditions, where longitudinal diffusion can be ignored, this equation reduces to

$$\mathrm{d}cG/\mathrm{d}t = \alpha - \beta\,cG. \qquad (4.6)$$

We assume that, except at points of photoisomerization, the hydrolysis rate 'constant' β is at all times constant throughout the outer segment, at its dark resting level β_{dark}, i.e. that

$$\beta(x, t) = \beta_{\text{dark}} \quad \text{(except at points of isomerization).} \tag{4.7}$$

At each point of isomerization the number of activated PDE* subunits is obtained from eqn (3.1) or (3.3), and the increase in hydrolytic activity is obtained from eqn (4.3).

The cyclase rate α is known to depend strongly on Ca_i^{2+} (Hodgkin & Nunn, 1988; Koch & Stryer, 1988). Over the rising phase of the response, however, we may simply approximate α as a constant, on the assumption that Ca_i^{2+} will change very little at early times; for the validity of this assumption see p. 733, and Cobbs & Pugh (1987). Thus, for flashes presented from darkness, we have

$$\alpha \approx \alpha_{\text{dark}} = \beta_{\text{dark}} \, cG_{\text{dark}}. \tag{4.8}$$

Pugh & Lamb (1990) review the evidence indicating that in the dark resting state the free and bound concentrations of cyclic GMP in darkness are $cG_{\text{dark}} \approx 4\,\mu\text{M}$ and $cG_{\text{bnd}} \approx 60\,\mu\text{M}$.

Step 5: Channel activity and outer segment current

Channel activity

The action of cyclic GMP in opening ion channels in the plasma membrane has been reviewed by Owen (1987), Yau & Baylor (1989) and Pugh & Lamb (1990). The probability p_{open} of a channel being open may be described by

$$p_{\text{open}}/p_{\text{max}} = \frac{(cG/K_{\text{d}})^n}{1 + (cG/K_{\text{d}})^n}, \tag{5.1}$$

where p_{open} and cG are functions of x and t. The apparent dissociation constant is $K_{\text{d}} \approx 17\text{--}30\,\mu\text{M}$, and the co-operativity index is $n = 2\text{--}3$ (Fesenko, Kolesnikov & Lyubarsky, 1985; see Yau & Baylor, 1989). The maximum open probability p_{max} has been reported to range from 0·1 to 0·45 with a mean of 0·3 (Matthews & Watanabe, 1988), so that even at a saturating concentration of cyclic GMP the channels are open for only a finite fraction of the time.

It has been shown that the reaction of cyclic GMP with the channels occurs within milliseconds (Cobbs & Pugh, 1987; Karpen , Zimmerman, Stryer & Baylor, 1988); see also review by Owen (1987) and the single-channel burst duration measurements of Matthews & Watanabe (1988). Accordingly, for our present purposes, we shall assume that eqn (5.1) applies instantaneously. However, in the future, to deal with the onset phase of responses to extremely bright flashes it is likely to be necessary to include explicit consideration of channel closure kinetics.

Since the concentration of cyclic GMP does not normally exceed its resting dark level of $cG_{\text{dark}} \approx 4\,\mu\text{M}$, and as $K_{\text{d}} \approx 17\text{--}30\,\mu\text{M}$, we have $cG \ll K_{\text{d}}$, so that under most conditions

$$p_{\text{open}}/p_{\text{max}} \approx (cG/K_{\text{d}})^n. \tag{5.2}$$

Outer segment current

In order to determine the current flowing into the outer segment we shall assume that the current–voltage relation of the light-sensitive conductance is instantaneous (reviewed in Owen, 1987; Yau & Baylor, 1989), and that the membrane voltage V is uniform throughout the outer segment. We denote the current density through the light-sensitive channels as $J(x,t)$ and write

$$J(x,t) = \frac{p_{\mathrm{open}}(x,t)}{p_{\mathrm{max}}} J_{\mathrm{max}}(V), \tag{5.3}$$

where $J_{\mathrm{max}}(V)$ is the maximum current density through the light-sensitive conductance at very high concentrations of cyclic GMP ($ca -5\ \mathrm{pA}\ \mu\mathrm{m}^{-2}$; Yau & Baylor, 1989; Cameron & Pugh, 1990).

Over the whole outer segment, of length L and circumference c, the current $i(t)$ flowing through the light-sensitive channels will be

$$i(t) = \int_0^L J(x,t)\,c\,\mathrm{d}x. \tag{5.4}$$

Dark current and photocurrent

In order to avoid the complication of the cell's capacitive time constant we shall consider the voltage-clamped cell, with $\mathrm{d}V/\mathrm{d}t = 0$. Furthermore, since we have assumed that changes in $\mathrm{Ca}_{\mathrm{i}}^{2+}$ can be ignored during the early part of the response, it will also be permissible to ignore any contribution from the Na^+–Ca^{2+} exchange current; see Cobbs & Pugh (1987).

Using these simplifications we can substitute eqns (5.2) and (5.3) into eqn (5.4) to obtain i_{dark}, the current in darkness through the light-sensitive channels, as

$$i_{\mathrm{dark}} = A_{\mathrm{s}} J_{\mathrm{max}}(V_{\mathrm{dark}})\,(cG_{\mathrm{dark}}/K_{\mathrm{d}})^n, \tag{5.5}$$

where A_{s} is the membrane surface area. Here we have implicitly assumed that spatial variations in cG_{dark} may be ignored.

We now introduce two parameters describing the electrical response: the normalized circulating current $F(t)$, and its complement, the normalized photo-current $R(t)$, defined by

$$F(t) = \frac{i(t)}{i_{\mathrm{dark}}} = 1 - R(t). \tag{5.6}$$

Hence, for the approximation given in eqn (5.2), and under voltage-clamped conditions and ignoring changes in exchange current, we obtain the normalized photoresponse as

$$R(t) \approx 1/L \int_0^L \{1 - (cG(x,t)/cG_{\mathrm{dark}})^n\}\,\mathrm{d}x. \tag{5.7}$$

In the case that $cG(x,t)$ is uniform along the outer segment (i.e. independent of x), eqn (5.7) reduces to

$$R(t) = 1 - (cG(t)/cG_{\mathrm{dark}})^n. \tag{5.8}$$

This represents an extension of eqn (5.2) which is applicable when the fractional circulating current is identical with the fraction of open channels (relative to that in darkness).

Channel closure time. These equations do not allow for the short time taken for channels to close when the cyclic GMP concentration drops (see above). For calculating the response at very early times it will be necessary to convolve the right-hand side of eqn (5.7) or (5.8) with an appropriate short delay function.

Analytical solutions of the equations

In order to obtain the solution $R(t)$ we need first to solve eqn (4.5) or, under isotropic conditions, eqn (4.6). The light-induced increase in rate constant $\Delta\beta(t)$ required in those equations may be obtained from eqn (4.3). The cyclase rate α (and all the remaining parameters in the equations) may be taken to be constant at suitably early times in the light response. Initially we treat the isotropic case of bright flashes, where longitudinal gradients in concentration may be ignored. In Appendix B we examine the more difficult case of the single-photon response, where longitudinal diffusion must be analysed.

Isotropic case: bright flash response

For simplicity we shall treat the case in which the intensity is uniform along the outer segment, as occurs with transverse illumination. It is possible to show that longitudinal gradients of cyclic GMP will be negligible at intensities greater than $\Phi \approx 100$ isomerizations in amphibian rods, i.e. they are negligible for all saturating flashes. In the absence of longitudinal gradients the differential equation for free cyclic GMP concentration is given by eqn (4.6). This equation may be rewritten, with the term β expanded into the form $\beta(t) = \beta_{\text{dark}} + \Delta\beta(t)$ and with $\alpha = \alpha_{\text{dark}}$, as

$$\mathrm{d}cG(t)/\mathrm{d}t = [\alpha_{\text{dark}} - \beta_{\text{dark}} \, cG(t)] - \Delta\beta(t) \, cG(t). \tag{6.1}$$

We wish to solve eqn (6.1) in response to a time-dependent $\Delta\beta(t)$. In this equation the term $\alpha_{\text{dark}} - \beta_{\text{dark}} \, cG(t)$ is initially zero (see eqn (4.8)), and we shall determine the solution under conditions where the term remains negligible; later (p. 734) we comment on the range of validity of this approximation. Equation (6.1) thus reduces to the simple form

$$\mathrm{d}cG/\mathrm{d}t = -\Delta\beta(t) \, cG, \tag{6.2}$$

which has the solution

$$cG(t)/cG_{\text{dark}} = \exp\left[-\int_0^t \Delta\beta(t') \, \mathrm{d}t'\right] \tag{6.3}$$

where t' is a dummy variable. Substitution of eqn (6.3) into eqn (5.8) gives the bright flash response as

$$R(t) = 1 - \exp\left[-n\int_0^t \Delta\beta(t') \, \mathrm{d}t'\right]. \tag{6.4}$$

Substitution of $\Delta\beta(t)$. The increment in PDE rate constant $\Delta\beta(t)$ is directly proportional to the number of activated PDE subunits $PDE^*(t)$, which in turn is

directly proportional to the number of isomerizations Φ delivered to the outer segment at $t = 0$; see eqns (4.3) and (3.1). Thus $\Delta\beta(t)$ may be written as

$$\Delta\beta(t) = \Phi\, PDE^*_\phi(t)\, \beta_{\text{sub}}, \tag{6.5}$$

where $PDE^*_\phi(t)$ is the number of activated PDE subunits per isomerization (i.e. $PDE^*(t)/\Phi$). Substitution of eqn (6.5) into eqn (6.4) then yields the bright flash response as

$$R(t) = 1 - \exp\left(-\Phi\left[n\,\beta_{\text{sub}}\int_0^t PDE^*_\phi(t')\,\mathrm{d}t'\right]\right). \tag{6.6}$$

This equation predicts that, irrespective of the time course of $PDE^*(t)$ or the values of n or β_{sub}, the response–intensity relation at fixed times during the rising phase of the response should be of the exponential form $1 - \exp[-I\,k_2(t)]$ given in eqn (2), on p. 723. At any fixed time, $k_2(t)$ is a constant given by the term in square brackets in eqn (6.6). The prediction of this exponential form follows directly from the nature of the reactions in the cytoplasm, without the need to postulate (Lamb *et al.* 1981) that even at early times in the response each isomerization blocks all the channels over a restricted length of outer segment.

Substitution of $PDE^*_\phi(t)$. The time course of increase in PDE* subunits in response to a flash at $t = 0$ is given by eqn (3.1). Except at very early times this function rises as a 'delayed ramp', given by eqn (3.3), so that eqn (6.5) may be written as

$$\Delta\beta(t) = \Phi\, \nu_{\text{RP}}\, \beta_{\text{sub}}\, \text{ramp}(t - t_{\text{eff}}). \tag{6.7}$$

Substitution of this expression into eqn (6.4) yields the normalized response to saturating flashes as

$$R(t) = 1 - \exp\left\{-\tfrac{1}{2}\Phi\left[\nu_{\text{RP}}\beta_{\text{sub}}\, n\right](t - t_{\text{eff}})^2\right\}, \quad t > t_{\text{eff}}. \tag{6.8}$$

This equation indicates that, within the validity of the delayed ramp approximation, the rising phase of the response at any saturating intensity has a common *shape*, described by a 'delayed Gaussian' function of time. Responses at different intensity differ simply by a time-scaling about the time $t = t_{\text{eff}}$.

Since each of the parameters in square brackets in eqn (6.8) is a constant, we thus have an analytical solution for the saturating flash response, expressed in terms of 'basic' physical parameters: ν_{RP} is the rate of activation of PDE subunits by a single Rh*, β_{sub} is the hydrolytic rate constant of a single activated subunit of PDE, and n is the co-operativity index of channel opening by cyclic GMP. The product of these parameters, $\nu_{\text{RP}}\beta_{\text{sub}}\, n$, represents an important quantity having the dimensions of time^{-2}. We shall denote this quantity as τ_ϕ^{-2}:

$$\tau_\phi^{-2} = \nu_{\text{RP}}\beta_{\text{sub}}\, n = \frac{\nu_{\text{RP}}\,(\tfrac{1}{2}k_{\text{cat}}/K_{\text{m}})\, n}{V_{\text{cyto}}\, N_{\text{Av}}\, BP}, \tag{6.9}$$

and we shall refer to τ_ϕ as the characteristic time constant of transduction. With this definition eqn (6.8) becomes

$$R(t) = 1 - \exp\left\{-\tfrac{1}{2}\Phi\left[\frac{t - t_{\text{eff}}}{\tau_\phi}\right]^2\right\}, \quad t > t_{\text{eff}}. \tag{6.10}$$

This simple expression should be applicable throughout most of the rising phase of responses obtained with saturating flashes. At very early times (for $t \approx t_{\text{eff}}$) eqn (3.3) is a poor approximation, but this will only create a significant problem in the case of extremely intense flashes; see p. 726.

Single-photon response

In Appendix B we deal with the single-photon case, which is complicated by longitudinal diffusion of cyclic GMP within the outer segment cytoplasm. We obtain the approximate solution for the normalized single-photon response $R_\phi(t)$ at early times as

$$R_\phi(t) \approx \frac{1}{2}\left[\frac{t - t_{\text{eff}}}{\tau_\phi}\right]^2, \quad t > t_{\text{eff}}. \tag{6.11}$$

This is the same approximation as is obtained from eqn (6.10) at early times with $\Phi = 1$. Thus, for small signals, the solution obtained by considering longitudinal spread is independent of the longitudinal diffusion coefficient D_x, and is identical with the solution obtained in the isotropic case.

Slope of the response to saturating flashes

From eqn (6.10) it may be shown (by setting the second derivative equal to zero) that the photoresponse attains its maximal slope (its inflexion point) at a time t_{infl} given by

$$t_{\text{infl}} - t_{\text{eff}} = \tau_\phi \, \Phi^{-\frac{1}{2}} \tag{6.12}$$

(where Φ is expressed in units of isomerizations per outer segment). The magnitude of this maximal slope is given by

$$\left[\frac{dR(t)}{dt}\right]_{\text{max}} = e^{-\frac{1}{2}}\tau_\phi^{-1}\Phi^{\frac{1}{2}}, \tag{6.13}$$

and it occurs when the photoresponse crosses the level

$$R(t_{\text{infl}}) = 1 - e^{-\frac{1}{2}} = 0{\cdot}393. \tag{6.14}$$

Furthermore, the tangent line at the point of maximal slope extrapolates back to a value at $t = t_{\text{eff}}$ given by

$$R(t_{\text{eff}}) = 1 - 2e^{-\frac{1}{2}} = -0{\cdot}213. \tag{6.15}$$

The interpretation of eqns (6.12)–(6.15) is as follows. For saturating flashes the interval $t_{\text{infl}} - t_{\text{eff}}$ to the occurrence of the maximal slope decreases, and the magnitude of the maximal slope increases, as the square root of the flash intensity. The maximal slope occurs when the normalized response crosses a fixed level close to 40%, irrespective of intensity, and the tangent lines for different intensities all intersect at time $t = t_{\text{eff}}$, and at a level about 21% beyond the dark current level, i.e. at $F(t_{\text{eff}}) = 1{\cdot}213$. Note, however, that these predictions do not apply at low intensities, since eqn (6.10) was derived for the isotropic case with bright flashes.

Range of validity of the solutions

Below we briefly outline the limitations on the accuracy of the above analytical solutions of our model.

Neglect of inactivation. The main limitation will arise from our neglect of the inactivation reactions: inactivation of Rh*, hydrolysis of the terminal phosphate of the $G_\alpha^* \cdot GTP$, and the accelerated cyclase rate brought about by lowered Ca_i^{2+}. The fastest of these reactions is likely to be the cyclase acceleration. With bright flashes the reduction in calcium concentration has a time constant of *ca* 0·5–2 s (reviewed in McNaughton, 1990; Pugh & Lamb, 1990). Because of the approximately inverse fourth-power relation between Ca_i^{2+} and cyclase activity (Koch & Stryer, 1988), the increase in cyclase rate will become significant within about 0·1 s. However, with bright flashes the rate constant $\beta(t)$ will have increased greatly by this time, and will dominate the rising phase of the response. With dim flashes, the reduction in Ca_i^{2+} is likely to be smaller, and will not have a significant effect until somewhat later in the response. Nevertheless, by the time of the inflection point in the rise of the real response to a dim flash (*ca* 0·4–0·5 s), neglect of inactivation will certainly be expected to influence the solution.

Spatial gradients. It may be shown that the assumption of isotropy causes little error for flashes of > 100 isomerizations.

Extremely intense flashes. For flashes delivering more than *ca* 10^5 isomerizations, neighbouring reactions in the disc membrane overlap significantly, so that the basis for eqn (A 1) disappears, and linearity with intensity is no longer expected. In addition, the need to consider very early times invalidates the delayed ramp approximation of eqn (3.3).

Approximation of eqn (6.2). Analytical and numerical methods show that the approximation employed in writing eqn (6.2) has negligible effect on the bright flash response; see e.g. Fig. 8.

Thus we expect our model to be accurate for the whole of the rising phase of responses to saturating flashes (for $\Phi < 10^5$ isomerizations), and for the first few hundred milliseconds of responses to dimmer flashes.

Inverse relation, for $\beta(t)$ from circulating current

In deriving eqn (6.4) we expressed the photocurrent in terms of $\beta(t)$, but it is straightforward to invert the argument to obtain $\beta(t)$ from the circulating current $F(t)$ during the bright flash response. Equations (4.6) and (5.8) may be re-arranged as

$$\beta(t) = \left[\beta_{dark} - \frac{d}{dt}(cG/cG_{dark})\right]/(cG/cG_{dark}), \tag{6.16}$$

and

$$cG/cG_{dark} = F(t)^{1/n}. \tag{6.17}$$

Substitution of eqn (6.17) into (6.16) thus gives

$$\Delta\beta(t) = -\frac{1}{n}\left[\frac{1}{F}\frac{dF}{dt}\right] + \beta_{dark}(F^{-1/n} - 1). \tag{6.18}$$

Note that at early times the term $\beta_{dark} (F^{-1/n} - 1)$ is zero, since $F(t) = 1$ at $t = 0$. Hence an approximation to $\Delta\beta(t)$ may be obtained from $F(t)$ without knowledge of β_{dark}. Comparison of eqns (6.7), (6.9) and (6.18) shows that the characteristic time constant τ_ϕ can be extracted from the slope of $\beta(t)$ in a form which is independent of n, as

$$\tau_\phi^{-2} \approx \frac{n \, d\beta/dt}{\Phi} \approx \frac{1}{\Phi} \frac{d}{dt} \left[-\frac{1}{F} \frac{dF}{dt} \right]. \tag{6.19}$$

Equation (6.18) is closely analogous to eqn (22B) of Hodgkin & Nunn (1988), which was applied by them to determine β in response to stepping the rod to Li^+-substituted Ringer solution. In the present study eqns (6.18) and (6.19) form the basis of the method used to estimate $\Delta\beta(t)$ and τ_ϕ^{-2} from photoresponses to bright flashes. These equations could equivalently be written in terms of $\ln F$, using the relation that $(dF/dt)/F = d(\ln F)/dt$.

RESULTS

We shall begin by applying the analytical 'inverse' technique (i.e. eqns (6.18)–(6.19)) to recordings of photocurrent, in order to determine the light-induced activation of PDE rate constant $\beta(t)$. Thereafter we shall compare the predictions of the 'forward' approach (i.e. eqns (6.7)–(6.15)) with electrical responses to flashes of light. Because of the existence of a wealth of electrical recordings from photo-receptors, obtained in previous work in our two laboratories, it has not been necessary to perform new experiments. Instead we have analysed existing recordings (available in digital or analog form) from the experiments of Torre, Matthews & Lamb (1986) and Cobbs & Pugh (1987); see legends to Figs 3–9 for details.

$\beta(t)$ calculated from the photocurrent

Application of the inverse method to the determination of $\beta(t)$ from the rising phase of the photocurrent is illustrated for two rods in Figs 3 and 4. In both figures the upper and middle panels plot families of photocurrents in response to flashes of increasing intensity, on slow and faster time bases. These responses have been normalized to the circulating dark current, and therefore represent $F(t)$. The lower panels illustrate the curves for $\Delta\beta(t)$ (i.e. $\beta(t) - \beta_{dark}$) calculated using eqn (6.18) with $n = 3$ and $\beta_{dark} = 0.5 \, s^{-1}$; this value was adopted from the measurements of Hodgkin & Nunn (1988) who obtained $n\beta_{dark} = 1.5 \, s^{-1}$. With this value of β_{dark}, the second term in eqn (6.18) was negligible except at the lowest intensities.

The cell in Fig. 3 was recorded with a suction pipette by Torre *et al.* (1986; their Fig. 2), and was stimulated with 21 ms flashes delivering from 10 to 2000 isomerizations. The cell in Fig. 4 was recorded under voltage clamp by Cobbs & Pugh (1987; their Fig. 2), and was stimulated with 22 ms flashes delivering from 70 to 7000 isomerizations. In accordance with the predictions of eqn (3.3), straight lines have been fitted to the curves of $\Delta\beta(t)$ in the lower panels of both figures, subject to the constraint that for each cell they intersect the abscissa at a common time. The lines provide a reasonable fit to the curves, indicating that $\Delta\beta(t)$ rises approximately as a delayed ramp.
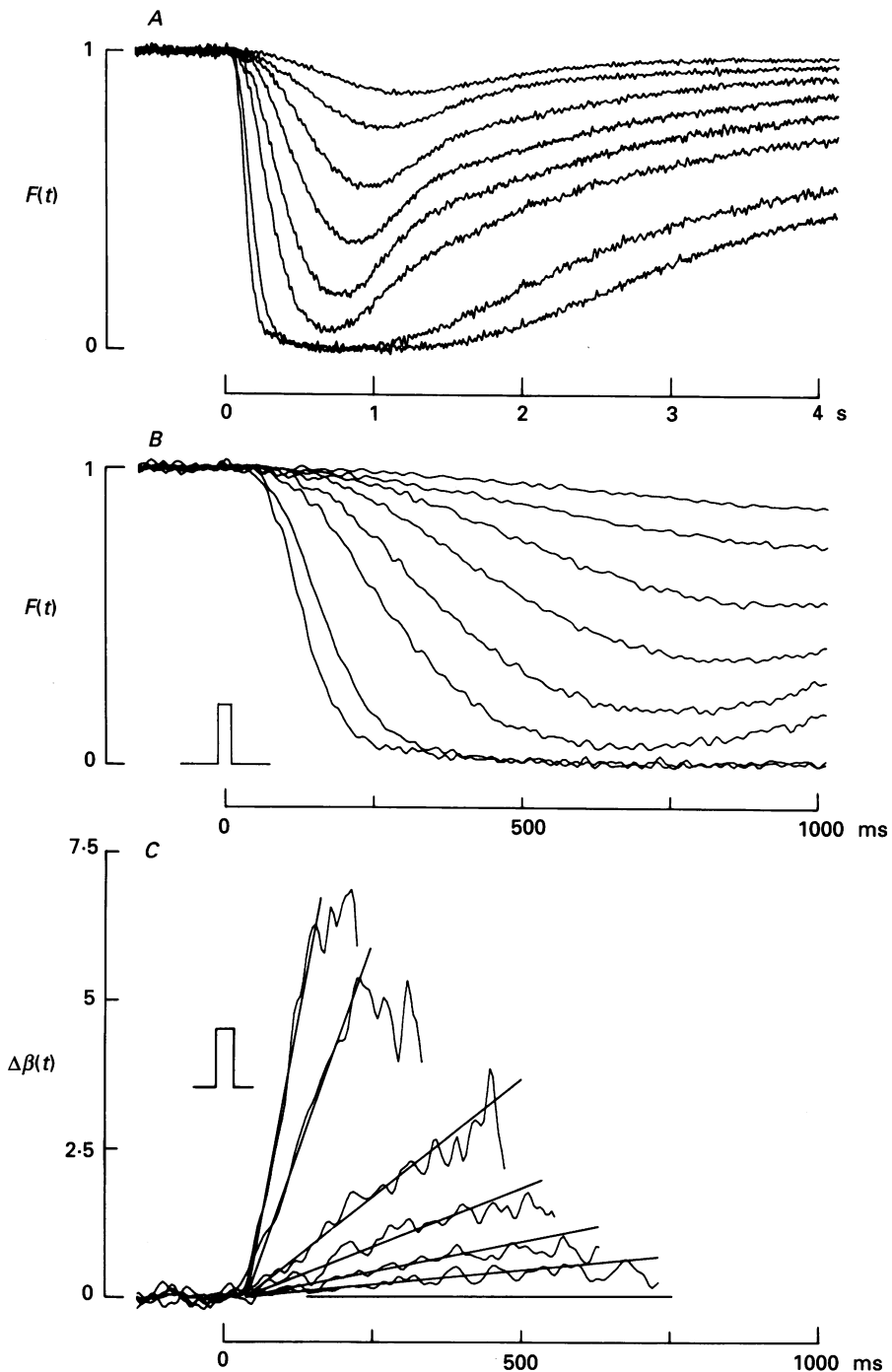
Fig. 3. Photocurrent responses and calculated increment in PDE rate constant $\Delta\beta(t)$ for a salamander red rod recorded with a suction pipette (i.e. unclamped). Panels A and B plot the normalized circulating current $F(t)$ at slow and faster time bases, while panel C plots the increment in rate constant $\Delta\beta(t)$ calculated using eqn (6.18), at all except the lowest two intensities. To test the prediction of eqn (3.3), straight lines have been fitted

Delay

The position of the common intercept (relative to the mid-point of the flash) provides an estimate of the sum of t_{eff} and the filtering delay in the two cases. For the unclamped cell in Fig. 3 the low-pass analog filtering contributed a delay of *ca* 10 ms; hence the intercept at *ca* 40 ms indicates that the sum of the transduction delay t_{eff} and the cell's electrical time constant was *ca* 30 ms. For the voltage-clamped cell in Fig. 4 the low-pass analog filtering contributed a delay of just 2·6 ms, so that the intercept at 19 ms indicates that the transduction delay was $t_{eff} \approx 16$ ms.

Slope

For the two cells, the fitted straight line at the highest intensity illustrated in each case had a slope $d\beta(t)/dt$ of 55 and 225 s^{-2}, at $\Phi = 1980$ and 7000 isomerizations respectively; note that since $\beta(t)$ is a 'rate' constant with units of s^{-1}, its slope has units of s^{-2}. Equation (6.19) shows that the characteristic time constant of transduction τ_ϕ can be obtained from the slope $d\beta/dt$, as $\tau_\phi^{-2} = (n\,d\beta/dt)/\Phi$, giving τ_ϕ values of 3·5 s and 3·2 s for the two cells. The rate ν_{RP} of activation of PDE* per isomerization can also be derived in this way, provided that β_{sub} is known. Equation (6.9) gives $\nu_{RP} = \tau_\phi^{-2}/(n\,\beta_{sub})$, so that substitution of $n = 3$ and $\beta_{sub} \approx 6 \times 10^{-6}$ s^{-1} (see Appendix C) yields $\nu_{RP} \approx 4600$ and 5400 activated PDE* subunits s^{-1} per isomerization, for the two cells.

For flash intensities spanning the general range shown in Figs 3C and 4C (100–10000 isomerizations), we found qualitatively similar results from analysis of the responses of eight cells. In each case the curves for $\Delta\beta(t)$ initially rose approximately according to the delayed ramp equation. The magnitudes of the slopes obtained for these cells are presented subsequently in Fig. 6, but before interpreting these values we shall first describe the behaviour observed at higher intensities.

Behaviour at higher intensities

Photocurrents and calculations of $\beta(t)$ are illustrated in Fig. 5 for another cell exposed to considerably higher intensities. For these traces the dark value β_{dark} is negligible, so that $\Delta\beta(t)$ and $\beta(t)$ may be considered to be equivalent. In this experiment the cell was voltage-clamped and the records have been filtered at a higher cut-off frequency in order to avoid limitations imposed by the cell's capacitive time constant or by the analog filtering; the Gaussian digital filter (see legend) caused no additional time delay. The upper panel plots traces of $F(t)$ from the cell illustrated in Fig. 8A of Cobbs & Pugh (1987), for 20 μs flashes at time $t = 0$, estimated to have

---

to the $\Delta\beta(t)$ curves, subject to the constraint that they intersect the abscissa at a common time. Cell from Fig. 2 of Torre *et al.* (1986); maximum current 44 pA; 21·6 °C. Traces filtered DC to 40 Hz, which gave an effective delay of 10 ms; sampling interval 5 ms; no Gaussian filtering. Flashes of 21 ms duration delivered: $\Phi = 9, 19, 38, 76, 145, 305, 1070$ and 1980 isomerizations. The gradient dF/dt in eqn (6.18) was determined by a linear regression fit over an N-point window centred at the time of interest; for this cell $N = 11$ points. The fitted lines have slopes of 0·95, 1·95, 3·9, 7·8, 28·5 and 54·8 s^{-2}, and intersect the abscissa 40 ms after the mid-point of the flash; this interval includes the analog filtering delay and the cell's capacitive time constant.
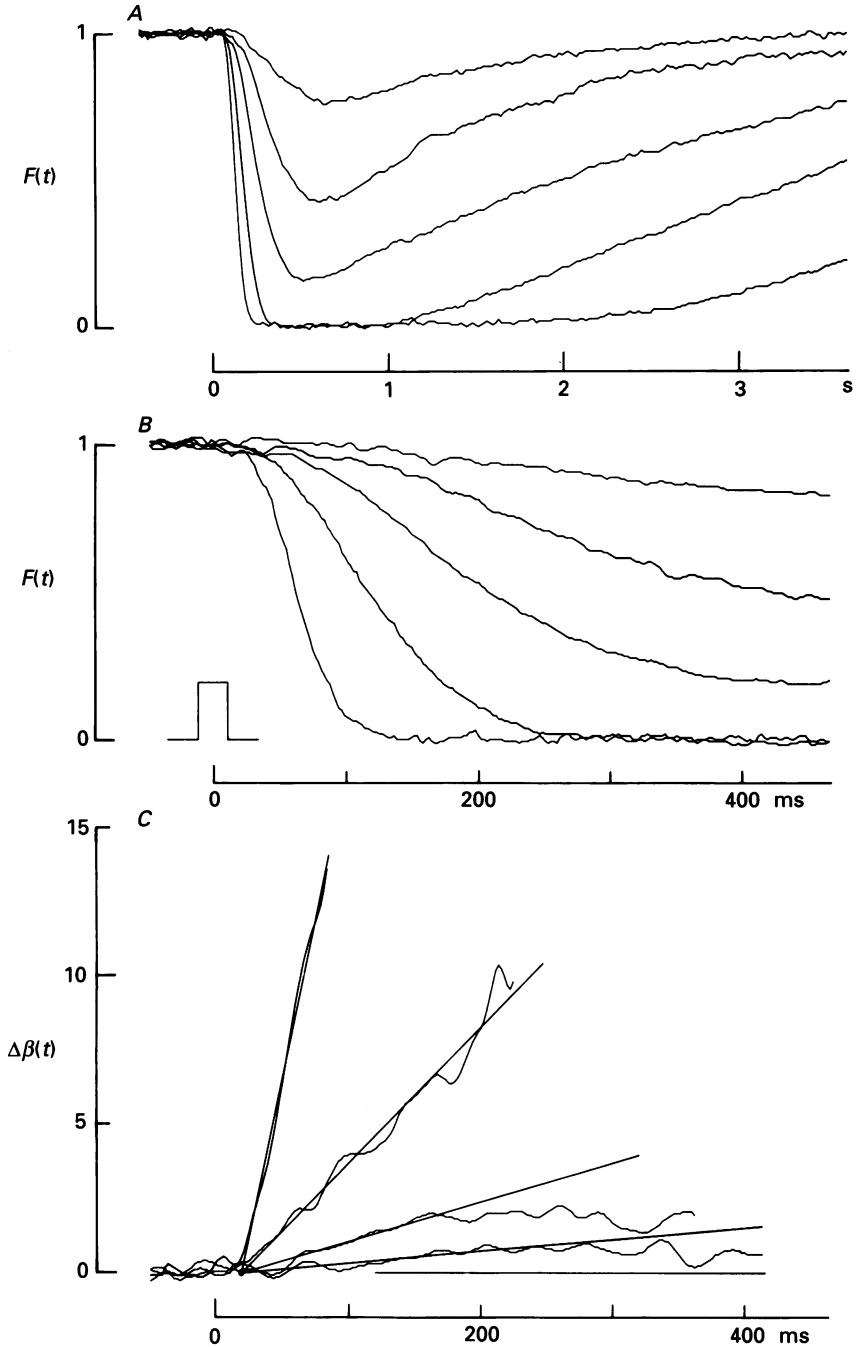
Fig. 4. Photocurrent responses and calculated increment in PDE rate constant $\Delta\beta(t)$ for a voltage-clamped salamander red rod. Details as for Fig. 3, except as follows. Cell from Figs 1 and 2 of Cobbs & Pugh (1987); maximum current 58 pA; 22·5 °C. Traces in A filtered DC to 15 Hz. Traces in B and C filtered DC to 150 Hz, which gave an effective delay of 2·6 ms; also Gaussian filtered at 25 Hz; sampling interval 2·2 ms. Flashes of 22 ms duration delivered: $\Phi = 70$, 220, 700, 2200 and 7000 isomerizations. The $\Delta\beta(t)$ calculations are for the brightest four of these; the gradient was fitted over $N = 7$ points.

delivered $2 \cdot 5 \times 10^4$, $2 \cdot 5 \times 10^5$, $2 \cdot 5 \times 10^6$ and $1 \cdot 6 \times 10^8$ isomerizations. The lower panel plots $\beta(t)$ calculated from the curves in the upper panel according to eqn (6.18), using $n = 3$.

Straight lines have been fitted to the traces in Fig. 5B. At an intensity of 25 000 isomerizations the intercept with the abscissa occurs at *ca* 13 ms, and at higher intensities the intercepts occur at earlier times. Such behaviour indicates break-down of the simple 'delayed ramp' approximation for $PDE^*(t)$ in which t_{eff} is assumed to be independent of intensity. The straight lines provide a reasonable fit, and the value of the intercept for 25 000 isomerizations indicates that $t_{\text{eff}} \approx 13$ ms in this case (since the filter delay was only 0·26 ms).

Dependence of the slope of $\beta(t)$ on flash intensity

A further prediction of eqn (3.1) or (6.5) is that the slope of the fitted lines in Figs 3–5 should scale in direct proportion to flash intensity. In the case of Fig. 5 the slopes of the lines at the first three intensities are in the ratio $1:8 \cdot 1:23$, while the flash intensities were in the ratio $1:10:100$; this suggests that linearity breaks down above *ca* 10^5 isomerizations.

The prediction of linearity with intensity may be examined by plotting $n\,(\mathrm{d}\beta/\mathrm{d}t)/\Phi$ against flash intensity Φ. If $\beta(t)$ is proportional to Φ, then this function should not vary with intensity, and this prediction is tested in Fig. 6. The factor n is included in order to render the plotted function independent of any parameters of the model. Equation (6.19) shows that $n\,(\mathrm{d}\beta/\mathrm{d}t)/\Phi$ may be obtained directly from $F(t)$ as

$$\frac{1}{\Phi}\frac{\mathrm{d}}{\mathrm{d}t}\left[-\frac{1}{F}\frac{\mathrm{d}F}{\mathrm{d}t}\right],$$

and that it is equivalent to τ_ϕ^{-2}. The rate ν_{RP} of activation of PDE* subunits per Rh* may be found from this parameter, if the value of β_{sub} is known; see eqn (6.9). Hence we also present a second ordinate scale on the right-hand side of Fig. 6, giving the rate ν_{RP} based on an assumed value of $\beta_{\text{sub}} = 6 \times 10^{-6}$ s^{-1} (Appendix C).

Results from fifteen salamander rods are collected in the double logarithmic plot of Fig. 6, where straight lines join symbols for individual cells. Filled symbols represent voltage-clamped recordings, while open symbols represent suction pipette recordings. Up to an intensity of about 10 000 isomerizations it appears that τ_ϕ^{-2} (or equivalently, ν_{RP}) estimated in this way is independent of flash intensity. This implies that the slope $\mathrm{d}\beta/\mathrm{d}t$ in plots of the kind of Figs 3–5 is directly proportional to Φ up to that intensity. The mean value of τ_ϕ^{-2} for all intensities up to 10 000 isomerizations was $0 \cdot 076 \pm 0 \cdot 015$ s^{-2} (S.D.; thirteen cells, at fifty-one intensities in all); this corresponds to $\tau_\phi = 3 \cdot 6 \pm 0 \cdot 4$ s (eqn (6.19)). For $\beta_{\text{sub}} \approx 6 \times 10^{-6}$ s^{-1} and $n = 3$ this corresponds to a mean PDE activation rate of $\nu_{\text{RP}} \approx 4200 \pm 800$ PDE* subunits s^{-1} per Rh*.

The fitted lines have slopes of 4·3, 12·2, 47·8 and 225 s^{-2}, and intersect the abscissa 19 ms after the mid-point of the flash. The numbers of isomerizations here and subsequently have been reduced by 0·262 log units from those given by Cobbs & Pugh (1987), to correct for an error in the value of extinction coefficient for porphyropsin used in that paper.

Value from Hodgkin & Nunn (1988)

Also included in Fig. 6 is a value, marked by an asterisk, obtained from the experiments of Hodgkin & Nunn (1988) at the one intensity for which we could determine the slope of the rising phase of their $\beta(t)$. They measured the rate of decay
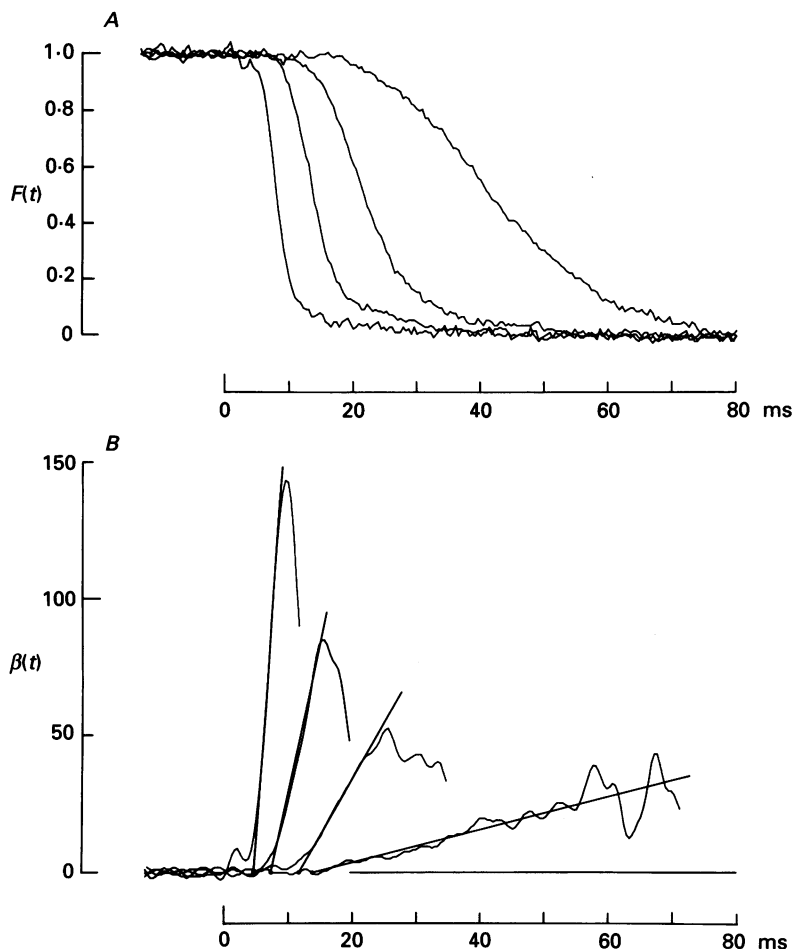

Fig. 5. Voltage-clamped photocurrent, and calculated PDE rate constant $\beta(t)$, for brighter flashes. *A*, normalized circulating current $F(t)$. *B*, $\beta(t)$ calculated from the traces in *A* using eqn (6.18); note that β_{dark} is negligible here, so that $\beta(t) \approx \Delta\beta(t)$. Salamander red rod from Cobbs & Pugh (1987), Fig. 8*A*: maximum current 82 pA; 22·5 °C; 20 μs flashes delivered $\Phi = 2·5 \times 10^4$, $2·5 \times 10^5$, $2·5 \times 10^6$ and $1·6 \times 10^8$ isomerizations. Bandwidth DC to 1500 Hz (giving a delay of 0·26 ms); Gaussian filtered at 200 Hz; sampling interval 440 μs. Slopes of the lines in *B* are 600, 4840, 14000 and 30000 s^{-2}.

of the light-sensitive current upon a rapid jump into Li$^+$-substituted Ringer solution, and they calculated $-(\mathrm{d}F/\mathrm{d}t)/F$ as in the first term of eqn (6.18). With Li$^+$ exposure they assumed that Ca$_i^{2+}$ rose rapidly, so that the cyclase was rapidly disabled (i.e. $\alpha = 0$). In this way they were able to estimate β at various times after a light stimulus.

From their Fig. 11 we measured the slope of their plot of $b(t)$ (i.e. $db/dt = d/dt\{-(dF/dt)/F\}$, equivalent to our $n\,d\beta/dt$) to be $11\cdot6$ s^{-2} at their intensity of $\Phi = 143$ isomerizations; this gives $(n\,d\beta/dt)/\Phi = 0\cdot081$ s^{-2}, virtually identical to our independent measurements of the same parameter by a different approach.
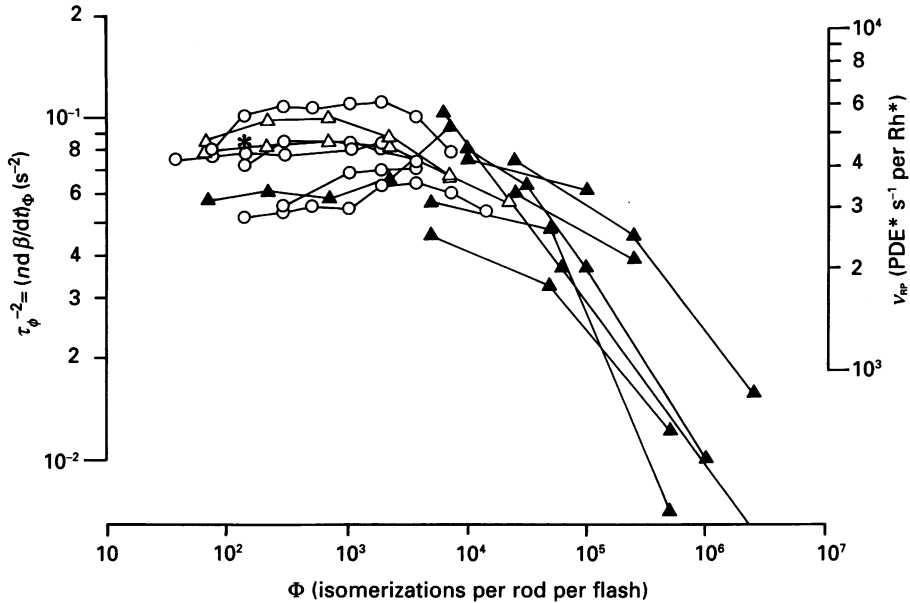

Fig. 6. Dependence of the calculated τ_ϕ^{-2} (or ν_{RP}) on flash intensity, for salamander red rods. The slope $d\beta/dt$ of responses such as those in Figs 3–5 has been measured, and converted to τ_ϕ^{-2} and ν_{RP}. The left ordinate is scaled in raw units of $(nd\beta/dt)/\Phi = \tau_\phi^{-2}$ (see eqn (6.19)), while the right ordinate has been converted to ν_{RP} using the estimated value of $\beta_{sub} = 6 \times 10^{-6}\,s^{-1}$ (see eqn (6.9) and Appendix C). Filled symbols are from eight cells recorded under voltage clamp; open symbols are from seven cells recorded with a suction pipette (free cells); values for each cell are joined by straight lines. Circles, from recordings of Torre *et al.* (1986); triangles, from recordings of Cobbs & Pugh (1987). The data point marked by an asterisk was obtained from Fig. 11 of Hodgkin & Nunn (1988); see text.

Dependence of delay time on flash intensity

The time delay t_{eff} preceding the rampwise increase in $\beta(t)$ could only be estimated reliably for voltage-clamped cells presented with moderately bright flashes. In the lowest intensity region at which we could measure the delay accurately (5000 to 25000 isomerizations), the mean value of t_{eff} was $16\cdot1 \pm 2\cdot0$ ms (S.D., seven cells; results not shown). Although the value decreased at higher intensities (with a slope of roughly 2 ms per log unit of intensity), there was no evidence to suggest that the true value of t_{eff} at low intensities exceeded 15–20 ms.

Deviation of $\beta(t)$ from linearity

In Fig. 6 it is clear that a marked decline in $(nd\beta/dt)/\Phi$ occurs at intensities above about 20000 photoisomerizations. In addition to this breakdown in linearity between $d\beta/dt$ and intensity, two kinds of deviation from the predicted rampwise increase

in $\beta(t)$ were also observed. It was found as a general feature (see Figs 3 and 5) that, following the initial approximately linear rise in $\beta(t)$, a distinct fall occurred. Furthermore it was also found (especially at high intensities) that the rise in $\beta(t)$ often appeared to taper off from its initial slope, and the calculated value of $\beta(t)$ seemed to asymptote towards a maximum (results not illustrated).

Non-linear behaviour of these kinds is not predicted by equation (3.1), but could arise from several mechanisms. Firstly, the effective buffering power BP may not be constant, but may instead increase as the free concentration of cyclic GMP drops; in Appendix C we find that when $F(t)$ has dropped to $1/8$, BP may approximately double. A second mechanism might involve the non-instantaneous closure of the cyclic GMP-gated channels. Recent power spectral measurements from excised patches exposed to cyclic GMP have shown a Lorentzian component with a time constant of *ca* 3 ms (V. Torre, M. Straforini & T. D. Lamb, personal communication) suggesting that the final tail of channel closure may be slower than previously assumed. A third relevant factor might involve competition for unreacted PDE, but calculations suggest that such an effect would only become significant at intensities considerably higher than those in Fig. 5. A fourth contributory factor might stem from alteration in the cytoplasmic GTP/GDP ratio, as GDP is released and GTP is consumed during the activation of the G-protein; but again, calculations suggest that this effect is likely to be minor during the rising phase.

Fit of the analytical solutions to the electrical response

Responses to dim flashes

We have compared the prediction of eqn (6.11) with the experimentally measured average response to very dim flashes, from our own experiments and those of others. A good example is provided by the response in Fig. 4 of Baylor *et al.* (1979). For the first 1 s of that response (not illustrated here) the waveform is well-fitted by the delayed parabola of eqn (6.11), with $\tau_\phi = 3\cdot1$ s and with a total delay of 50 ms (but the value of this delay is not critical). The total delay is made up of expected delays of approximately 10–20 ms for t_{eff}, 10–20 ms for the cell's electrical time constant, and approximately 15 ms for the low-pass analog filtering used. In this experiment the estimated number of photoisomerizations, $\Phi \approx 0\cdot53$, should be very accurate, since it was determined from measurement of the probability of obtaining a successful response in the 'photon counting' range (see Baylor *et al.* 1979).

We analysed the dim flash kinetics in published recordings from twenty studies in the literature, and found no reason to reject the fit of the delayed parabola of eqn (6.11); results not illustrated. At room temperature in lower species the mean value of τ_ϕ was $3\cdot4$ s for toad (five studies), slightly shorter than the mean of $4\cdot7$ s for salamander rods (seven studies). For cones from turtle and salamander the mean τ_ϕ was $1\cdot8$ s (two studies). At body temperature in mammals the mean τ_ϕ for both rods and cones was approximately $0\cdot5$ s (three and two studies).

Responses to families of flashes

Figure 7 illustrates responses of a salamander rod to a series of flashes of increasing intensity, replotted from the original recordings of Fig. 2 of Torre *et al.* (1986). The responses in Fig. 7*A* were obtained under control conditions, while those in Fig. 7*B*

were obtained after incorporation of the calcium buffer BAPTA (bis-(O-aminophenoxy) ethane-N,N,N',N' tetraacetic acid) into the cytoplasm. Because the presence of buffer greatly slows down changes in Ca_i^{2+}, the responses in Fig. 7B would be expected to reflect the transduction process with one of the mechanisms of
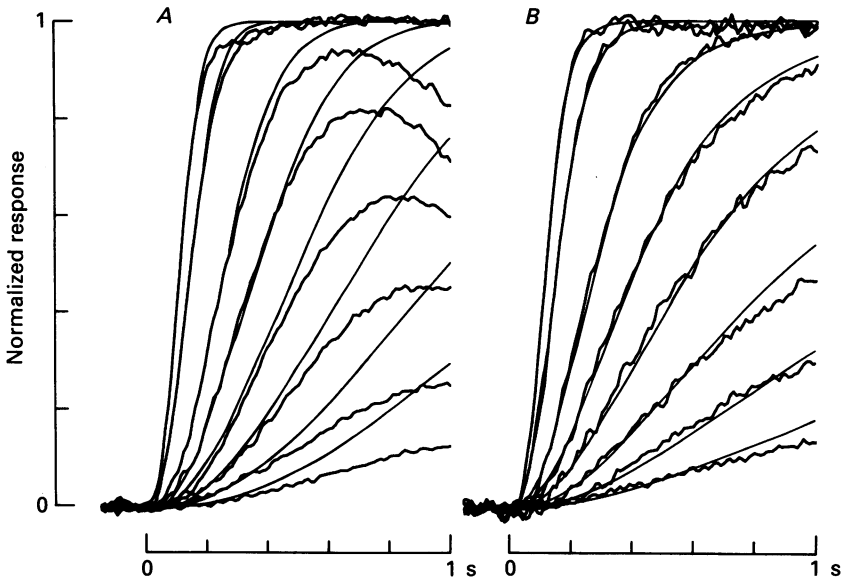

Fig. 7. Comparison of families of flash responses from a salamander rod with predictions of the model. The noisy traces are from Fig. 2 of Torre *et al.* (1986), for a salamander rod stimulated by flashes delivering from 9 to 1980 isomerizations. *A*, under control conditions. *B*, with the calcium buffer BAPTA trapped in the cytoplasm. Responses low-pass filtered at 20 Hz (6–pole Bessel), giving a delay of about 22 ms. The smooth curves were obtained as follows. On the left is plotted eqn (6.10) with $\tau_\phi = 3\cdot6$ s and $t_{eff} = 20$ ms; thus the total delay to onset of the PDE ramp was 42 ms from the mid-point of the flash. On the right is plotted the solution obtained by numerical integration of the differential eqn (4.6), substituted into eqn (5.8), with $\beta(t)$ obtained from eqn (6.7). Same values of τ_ϕ and t_{eff} as on the left, together with $\beta_{dark} = 2$ s^{-1} and $n = 3$. In an alternative procedure, curves for the right hand panel were calculated using $\beta_{dark} = 0\cdot5$ s^{-1}, with the addition of a first-order removal of the activated G-protein with time constant $0\cdot67$ s; those curves (not shown) were almost indistinguishable from the illustrated curves.

inactivation (altered calcium concentration) effectively disabled. As shown by Torre *et al.* (1986), the early rising phase of the response at any fixed intensity is common in the two cases, and the main difference between the two families is that the control responses begin, and complete, their recovery sooner.

The theoretical curves fitted to Fig. 7A were obtained from the simplest model, eqn (6.10). As in the fit to the dim flash response, only two parameters are involved: the characteristic time constant τ_ϕ (3·6 s in this rod) and the short delay t_{eff} (20 ms). In this figure, though, it is not just a single response, but the early part of the entire family of responses, which is fitted by the model with just two parameters. At times greater than about 200–300 ms, however, the theoretical curves systematically

depart from the experimental responses in Fig. 7*A*, presumably because of a combination of at least two factors: the onset of inactivation reactions in the real cell, and the approximations involved in the simple model.

The first of these factors can be minimized by examining responses obtained when the calcium concentration is buffered, as in the experimental traces in Fig. 7*B*. The
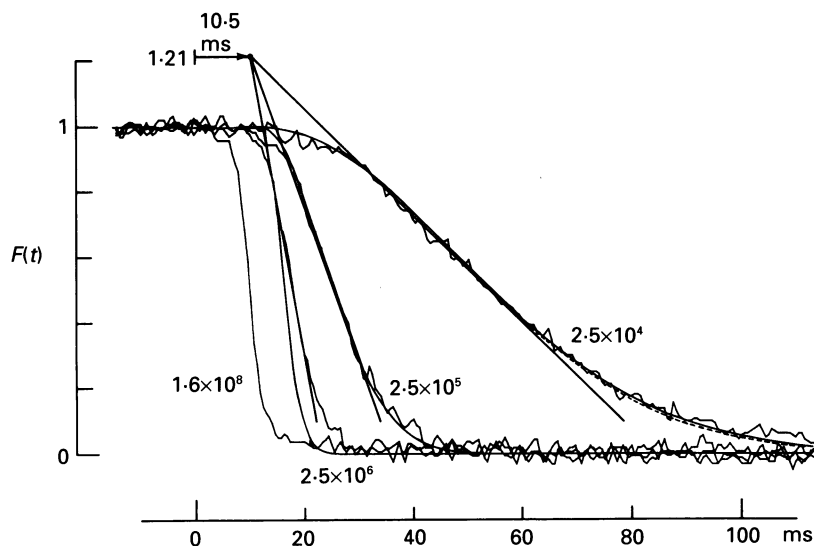

Fig. 8. Normalized circulating current $F(t)$ (noisy traces) for intense 20 μs flashes which delivered the indicated number of photoisomerizations at $t = 0$. Tangent lines from eqns (6.12)–(6.15), and analytical solutions from eqn (6.10), are drawn near the traces (except for the most intense flash). The common intercept of the tangents at $F = 1.213$ gives the effective delay time $t_{eff} \approx 10$ ms. For the lower two intensities, the tangent lines have slopes of 16.4 and 48.5 s^{-1} at $\Phi = 25000$ and 250000 isomerizations. At the lowest intensity, substitution into eqn (6.13) gives $\tau_\phi \approx 5.8$ s. The smooth curves plot the analytical solution eqn (6.10) for the lower three intensities, with $\tau_\phi = 5$ s and $t_{eff} = 9$ ms. At 25000 and 250000 isomerizations the fit to the experimental traces is good, but at 2.5×10^6 isomerizations the curve rises too quickly. Interrupted curves: numerical integration of eqn (4.6) with eqn (6.7), and substitution into eqn (5.8), using $\beta_{dark} = 1$ s^{-1} and $n = 3$; the interrupted curve can be distinguished from the continuous curve only at the lowest intensity.

second factor may be avoided by using numerical integration of eqn (4.6), rather than the simplified approach of eqn (6.2) which led to eqn (6.10). The theoretical curves illustrated in Fig. 7*B* were obtained by numerical integration (see legend), and provide a good description of the rising phase of the calcium-buffered responses out to almost 1 s, for intensities from about 10 to 2000 isomerizations.

Responses to intense flashes

Responses and predictions are compared in Fig. 8 at higher intensities, from 2.5×10^4 to 1.6×10^8 isomerizations. Superimposed tangents from our simplified theory (eqns (6.12)–(6.15)), fitted to the traces for the lower three intensities, appear to intersect roughly as predicted at $F \approx 1.21$, at a time of $t_{eff} \approx 10$ ms. Furthermore, the predicted time scaling according to $\Phi^{-\frac{1}{2}}$ also appears to hold, at least up to

250000 isomerizations: for a 10-fold increase in intensity, from 25000 to 250000 isomerizations, the slope of the tangent increased from 16·4 to 48·5 s^{-1}, a factor of 2·96, in comparison with the prediction of $\sqrt{10} = 3·16$.

Figure 8 also illustrates the theoretical curves predicted by the model at the lower three intensities. The continuous curves plot the delayed Gaussians of eqn (6.10),
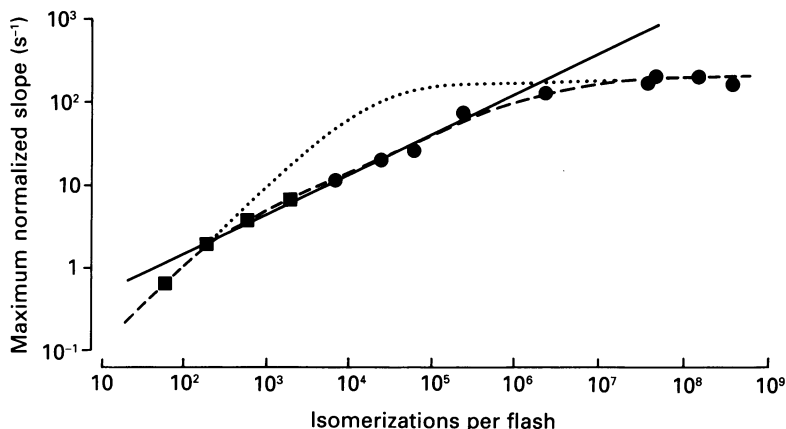

Fig. 9. Maximal slope of $F(t)$ over a wide range of intensities, from voltage-clamped salamander rods stimulated with 20 μs flashes. The points are replotted from Fig. 12 of Cobbs & Pugh (1987); ■, data from a single cell; ●, averages from at least four cells. The dotted and interrupted lines are respectively the Michaelis (hyperbolic) relation, and a curve drawn by eye, as fitted by Cobbs & Pugh (1987). The continuous straight line has a slope of 0·5 in these double logarithmic co-ordinates, and represents the square-root prediction of eqn (6.13); its position corresponds to a value of the characteristic time constant $\tau_\phi = 4·1$ s. The abscissa has been altered by 0·262 log units from that of Cobbs & Pugh (1987) to correct for an error in the value of extinction coefficient for the photopigment used in that paper.

with $\tau_\phi = 5·0$ s and $t_{\text{eff}} = 9$ ms, which provide a good fit to the experimental results at the lower two flash intensities, 25000 and 250000 isomerizations. Not unexpectedly, the fit of the simple model breaks down at intensities higher than 250000 isomerizations.

The interrupted curves in Fig. 8 plot the results of numerical integration of eqn (4.6), using the same values of τ_ϕ and t_{eff} as for the continuous curves, and with $\beta_{\text{dark}} = 1$ s^{-1}. The agreement between the continuous and interrupted curves is very close, and indeed the separate curves can only be distinguished at the lowest intensity ($\Phi = 25000$ isomerizations). In this plot we deliberately increased β_{dark} to 1 s^{-1}, in order to illustrate a difference between the curves; at the correct value of $\beta_{\text{dark}} = 0·5$ s^{-1} they were difficult to distinguish. This shows that the simplification in eqn (6.2) causes little error.

Slope of the bright flash response

In Fig. 9 the experimentally measured maximal slopes from Fig. 12 of Cobbs & Pugh (1987) are compared with the predictions of eqn (6.13). Over a range of at least three log units of intensity (from about 250 to around 250000 isomerizations) the slope closely obeys the square root prediction, given in these double logarithmic co-

ordinates by the straight line with slope 0·5. From the position of the line, τ_ϕ for these salamander rods is obtained from eqn (6.13) as approximately 4·1 s. Hence the model provides a simple but accurate analytical description of a further experimental result in the literature which has not previously been treated in theoretical terms.

DISCUSSION

Comparison of predictions with experiment

The theoretical predictions of the model were found to agree with experiment remarkably accurately:

Timecourse of PDE*(t). The effective rate constant $\beta(t)$ of cyclic GMP hydrolysis, which is proportional to $PDE^*(t)$, can be extracted from the normalized circulating current $F(t)$, using eqn (6.18): $\Delta\beta(t) \approx -(\mathrm{d}F/\mathrm{d}t)/nF$. As shown in Figs 3–5, the theoretical prediction that $\beta(t)$ should initially increase as a delayed ramp (eqn (3.3)) was indeed found to be obeyed. Over most of the time window for which $\beta(t)$ could be measured reliably (prior to substantial suppression of the circulating current) the rise in $\Delta\beta(t)$ was well-fitted by a straight line. For intensities up to *ca* 25 000 isomerizations the fitted lines intersected the abscissa at a common time, $t_{\text{eff}} \approx 15$ ms, termed the effective delay time.

Linearity of PDE*(t) with intensity. As also predicted by eqn (3.3), the slope of the fitted lines was very nearly proportional to flash intensity Φ, up to quite high intensities. This was tested by plotting (against flash intensity, in Fig. 6) the parameter $(n\,\mathrm{d}\beta/\mathrm{d}t)/\Phi$, which is equivalent to τ_ϕ^{-2}. Below about 10^4 isomerizations per flash, τ_ϕ^{-2} was independent of intensity, with a mean value of 0.076 ± 0.015 (s.d.) s^{-2}, corresponding to $\tau_\phi \approx 3.6$ s (for salamander rods at 22 °C). Even at an intensity of $\Phi \approx 2.5 \times 10^5$ isomerizations the value of the parameter had only fallen to about half.

Single-photon response. The initial rise of the response to a dim flash was well-fitted by a delayed parabola, as predicted by eqn (6.11). While this finding does not provide a strong test of the theory, it does provide a simple means to extract values for τ_ϕ from records in the literature.

Bright flash response. For bright flashes (Figs 7–8) the form of the recorded electrical response was well described over its whole rising phase by the 'delayed Gaussian' expression of eqn (6.10). Apart from the fixed short delay t_{eff}, the response family was completely characterized during the first few hundred milliseconds by the single parameter τ_ϕ, for intensities up to approximately $\Phi = 10^5$ isomerizations.

Maximum slope of photoresponse. The normalized maximum slope of the photocurrent varied with flash intensity in close agreement with the square-root prediction of eqn (6.13), for intensities from about 250–250 000 isomerizations.

Response–intensity relation. The exponential form of saturation predicted by the model (eqn (6.10)) has indeed been observed over the last decade in a variety of experiments, beginning with those of Lamb *et al.* (1981).

Extremely intense flashes. The kinetic predictions of the model were found to deviate significantly from experiment for flashes delivering more than about 250 000 isomerizations. Such deviation is not unexpected: the simple 'delayed ramp' description of the protein reactions is an approximation which will not be applicable

at early times when there are large numbers of isomerizations per disc; see pp. 727, 734.

Implications of the equations

Characteristic time constant of transduction

The overall gain of phototransduction may be expressed in terms of the single parameter τ_ϕ^{-2}, where we refer to τ_ϕ as the characteristic time constant of transduction. In eqn (6.9) this overall gain is expressed as the product of three underlying parameters: $\tau_\phi^{-2} = \nu_{RP}\beta_{sub}\, n$. These three parameters may be thought of as the gains of three separate processes: ν_{RP} is the overall gain linking rhodopsin isomerization to the activation of PDE subunits, β_{sub} is the hydrolytic gain linking activated PDE subunits to cyclic GMP concentration, and n is the gain linking cyclic GMP concentration to channel activity. Apart from the short delay t_{eff}, all that is needed to obtain the photoresponse is the parameter τ_ϕ^{-2} together with the intensity Φ (eqn (6.10)).

Rate of activation of PDE*(t)

The rate ν_{RP} of activation of PDE* subunits per Rh* may be found from τ_ϕ^{-2} using eqn (6.9). For $\tau_\phi^{-2} = 0.076 \pm 0.015$ s^{-2}, substitution of $n = 3$ and $\beta_{sub} \approx 6 \times 10^{-6}$ s^{-1} yields $\nu_{RP} = 4200 \pm 800$ PDE* s^{-1} per Rh*. Clearly the result of this calculation depends critically on the value we have adopted for β_{sub} (see Appendix C), and we stress that we have not been able to determine this unequivocally. Subject to this uncertainty, our results indicate that a single photoisomerization triggers the activation of PDE* subunits at a rate of about 3000–6000 s^{-1}.

For comparison, the diffusion limit on the rate of activation of the G-protein was calculated theoretically as $\nu_{RG} < 7000$ G* s^{-1} per Rh*. The main source of uncertainty in that limit was the value for the lateral diffusion coefficient D_G of the G-protein at the disc membrane surface. Since the upper limit on the coupling gain c_{GP} is about 0·9, the diffusion limit on the rate of activation of PDE subunits is about 7000×0.9, or $\nu_{RP} < 6300$ PDE* s^{-1} per Rh*. Hence, subject to the reliability of our estimates of β_{sub} and D_G, it appears that the PDE is activated at a substantial fraction of the limit which is theoretically possible for the pair of cascaded reactions (i.e. *ca* 4200/6300). We therefore conclude that it is likely that each of these protein activation steps proceeds at a rate that cannot be far short of its diffusion limit; see also Kahlert & Hofmann (1991).

Response–intensity relation

The exponential form of the observed response–intensity relation was originally taken as support for the occurrence of localized saturation, whereby all the channels are closed in a short region near the site of photon absorption (Lamb *et al.* 1981). However, eqn (6.6) indicates that the exponential form is expected as the inevitable consequence of the reactions known to occur in the cytoplasm, irrespective of the occurrence of longitudinal spread of excitation. Hence the exponential form cannot be taken as evidence supporting localized saturation (sometimes referred to as 'total occlusion').

Furthermore, our analysis of the single photon response in Appendix B shows that local saturation of channels will not occur to an appreciable extent during the first

500 ms of the response of amphibian rods at room temperature; see p. 756. In a salamander rod, for example, the analysis indicates that only about 10 % of the channels are closed at the point of isomerization 500 ms after the flash. This calculation depends of course on the value adopted for the effective longitudinal diffusion coefficient D_x of cyclic GMP in the cytoplasm. Recently Cameron & Pugh (1990) have estimated the diffusion coefficient directly, by incorporating cyclic GMP into the inner segment and measuring the induced outer segment current. The value they obtained for salamander rods was 3–10 μm^2 s^{-1} (mean 7 μm^2 s^{-1}), very close to the value estimated theoretically on the basis of the cytoplasmic buffering power and baffling by the discs (see Appendix C).

Time course of the photoresponse

The underlying t^2 rise in the response to an *impulse* implicates the intervention of $N = 3$ stages of pseudo-first-order delay in generation of the response; see Baylor *et al.* (1974). In our model these three integrating processes are identified as: (i) the step-wise activation of rhodopsin by a photon, (ii) the catalytic activation of G-protein by an Rh*, and (iii) the enzymatic hydrolysis of cyclic GMP by the activated PDE*. The link from G* to PDE* contributes only a short delay, which we have consolidated into the effective delay time t_{eff}.

Human rods

The interpretations may be extended to human rods *in vivo* through analysis of the electroretinogram (ERG). It has long been accepted that the a-wave of the ERG is associated with photoreceptor activity, and it seems likely that its time course is an accurate reflection of the suppression of the circulating rod current. Hood & Birch (1990) have recently investigated the early rise of the ERG in response to very brief (10 μs) flashes. Their Figs 8 and 9 indicate that the a-wave rises approximately as t^2 after an initial delay of *ca* 3 ms, although the authors in fact interpreted the rise as *ca* t^4 without allowance for a fixed delay; it is unclear what proportion of the *ca* 3 ms delay represents their analog filtering. The existence of an initial rise according to a delayed parabola suggests that our model also provides an accurate description of human rod activity. Taking their maximum response to have been 120 μV, and using the intensity conversion that 1 scotopic troland s equals 5 isomerizations per rod, the characteristic time constant for human rods is calculated as $\tau_\phi \approx 0.5$ s. This coincides very closely with the value we determined for photocurrents from other mammalian rods (p. 742).

Summary

In summary, our analysis provides a unifying theoretical framework for studying the responses of photoreceptors from different species, by capturing the fundamental gain of transduction in terms of a single parameter determined by the biochemical and physical properties of the outer segment.

REFERENCES

ABRAMOWITZ, M. & STEGUN, I. A. (1964). *Handbook of Mathematical Functions*. Dover Publications, New York.

BAUMANN, CH. (1978). The equilibrium between metarhodopsin I and metarhodopsin II in the isolated frog retina. *Journal of Physiology* **279**, 71–80.

BAYLOR, D. A., HODGKIN, A. L. & LAMB, T. D. (1974). The electrical response of turtle cones to flashes and steps of light. *Journal of Physiology* **242**, 685–727.

BAYLOR, D. A., LAMB, T. D. & YAU, K.-W. (1979). Responses of retinal rods to single photons. *Journal of Physiology* **288**, 613–634.

CAMERON, D. A. & PUGH, E. N. JR (1990). The magnitude, time course and spatial distribution of current induced in salamander rods by cyclic guanine nucleotides. *Journal of Physiology* **430**, 419–439.

CARSLAW, H. S. & JAEGER, J. C. (1959). *Conduction of Heat in Solids*. 2nd edn. Oxford University Press, Oxford.

CHABRE, M. (1985). Trigger and amplification mechanisms in visual transduction. *Annual Review of Biophysics and Biophysical Chemistry* **14**, 331–360.

CLEGG, R. M. & VAZ, W. L. C. (1985). Translational diffusion of proteins and lipids in artificial lipid bilayer membranes. In *Progress in Protein–Lipid Interactions*, ed. WATTS, A. & DE PONT, J. J. H. H. M., pp. 173–229. Elsevier, Amsterdam.

COBBS, W. H. & PUGH, E. N. JR (1987). Kinetics and components of the flash photocurrent of isolated retinal rods of the larval salamander, *Ambystoma tigrinum*. *Journal of Physiology* **394**, 529–572.

DETERRE, P., BIGAY, J., FORQUET, F., ROBERT, M. & CHABRE, M. (1988). cGMP phosphodiesterase of retinal rods is regulated by two inhibitory subunits. *Proceedings of the National Academy of Sciences of the USA*. **85**, 2424–2428.

FESENKO, E. E., KOLESNIKOV, S. S. & LYUBARSKY, A. L. (1985). Induction by cyclic GMP of cationic conductance in plasma membrane of retinal rod outer segment. *Nature* **313**, 310–313.

FORTI, S., MENINI, A., RISPOLI, G. & TORRE, V. (1989). Kinetics of phototransduction in retinal rods of the newt *Triturus cristatus*. *Journal of Physiology* **419**, 265–295.

GRAY-KELLER, M. P., BIERNBAUM, M. S. & BOWNDS, M. D. (1990). Transducin activation in electropermeabilized frog rod outer segments is highly amplified, and a portion equivalent to phosphodiesterase remains membrane-bound. *Journal of Biological Chemistry* **265**, 15323–15332.

GUPTA, B. D. & WILLIAMS, T.P. (1990). Lateral diffusion of visual pigments in toad (*Bufo marinus*) rods and in catfish (*Ictalurus punctatus*) cones. *Journal of Physiology* **430**, 483–496.

HAMM, H. E. & BOWNDS, M. D. (1984). A monoclonal antibody to guanine nucleotide binding protein inhibits the light-activated cyclic GMP pathway in frog rod outer segments. *Journal of General Physiology* **84**, 265–280.

HARGRAVE, P. A., HOFMANN, K. P. & KAUPP, U. B. (ed.) (1992). *Signal Transduction in Photoreceptor Cells*. Springer, Berlin.

HODGKIN, A. L. & NUNN, B. J. (1988). Control of light-sensitive current in salamander rods. *Journal of Physiology* **403**, 439–471.

HOFMANN, K. P. (1986). Photoproducts of rhodopsin in the disc membrane. *Photobiochemistry and Photobiophysics* **13**, 309–327.

HOOD, D. C. & BIRCH, D. G. (1990). The a-wave of the human electroretinogram and rod receptor function. *Investigative Ophthalmology and Visual Science* **31**, 2070–2081.

KAHLERT, M. & HOFMANN, K. P. (1991). Reaction rate and collisional efficiency of the rhodopsin–transducin system in intact retinal rods. *Biophysical Journal* **59**, 375–386.

KARPEN, J. W., ZIMMERMAN, A. L., STRYER, L. & BAYLOR, D. A. (1988). Gating kinetics of the cyclic GMP-activated channel of retinal rods: flash photolysis and voltage clamp studies. *Proceedings of the National Academy of Sciences of the USA* **85**, 1287–1291.

KOCH, K.-W. & STRYER, L. (1988). Highly cooperative feedback control of retinal rod guanylate cyclase by calcium ions. *Nature* **334**, 64–66.

KÜHN, H. (1984). Interactions between photoexcited rhodopsin and light-activated enzymes in rods. *Progress in Retinal Research* **3**, 123–156.

LAMB, T. D., McNAUGHTON, P. A. & YAU, K.-W. (1981). Spatial spread of activation and background desensitization in rod outer segments. *Journal of Physiology* **319**, 463–496.

LIEBMAN, P. A., PARKER, K. R. & DRATZ, E. A. (1987). The molecular mechanism of visual excitation and its relation to the structure and composition of the rod outer segment. *Annual Review of Physiology* **49**, 765–791.

LIEBMAN, P. A. & PUGH, E. N. JR (1979). The control of phosphodiesterase in rod disk membranes: kinetics, possible mechanisms and significance for vision. *Vision Research* **19**, 375–380.

MATTHEWS, G. & WATANABE, S.-I. (1988). Activation of single ion channels from toad retinal rod inner segments by cyclic GMP: concentration dependence. *Journal of Physiology* **403**, 389–405.

McNaughton, P. A. (1990). Light response of vertebrate photoreceptors. *Physiological Reviews* **70**, 847–883.

Naqvi, K. R. (1974). Diffusion-controlled reactions in two-dimensional fluids: discussion of measurements of lateral diffusion of lipids in biological membranes. *Chemical Physics Letters* **28**, 280–284.

Owen, W. G. (1987). Ionic conductances in rod photoreceptors. *Annual Review of Physiology* **49**, 743–764.

Penn, R. D. & Hagins, W. A. (1972). Kinetics of the photocurrent of retinal rods. *Biophysical Journal* **12**, 1073–1094.

Pugh, E. N. Jr & Cobbs, W. H. (1986). Visual transduction in vertebrate rods and cones: a tale of two transmitters, calcium and cyclic GMP. *Vision Research* **26**, 1613–1643.

Pugh, E. N. Jr & Lamb, T. D. (1990). Cyclic GMP and calcium: the internal messengers of excitation and adaptation in vertebrate photoreceptors. *Vision Research* **30**, 1923–1948.

Sneyd, J. & Tranchina, D. (1989). Phototransduction in cones: an inverse problem in enzyme kinetics. *Bulletin of Mathematical Biology* **6**, 749–784.

Stryer, L. (1986). Cyclic GMP cascade of vision. *Annual Review of Neuroscience* **9**, 87–119.

Torney, D. C. & McConnell, H. M. (1983). Diffusion-limited reaction rate theory for two-dimensional systems. *Proceedings of the Royal Society* A **387**, 147–170.

Torre, V., Matthews, H. R. & Lamb, T. D. (1986). Role of calcium in regulating the cyclic nucleotide cascade of phototransduction in retinal rods. *Proceedings of the National Academy of Sciences of the USA* **83**, 7109–7113.

Uhl, R., Wagner, R. & Ryba, N. (1990). Watching G proteins at work. *Trends in Neurosciences* **13**, 64–70.

Wensel, T. G. & Stryer, L. (1990). Activation mechanism of retinal rod cyclic GMP phosphodiesterase probed by fluorescein-labeled inhibitory subunit. *Biochemistry* **29**, 2155–2161.

Whalen, M. M., Bitensky, M. & Takemoto, D. (1990). The effect of the γ-subunit of the cyclic GMP phosphodiesterase of bovine and frog (*Rana catesbiana*) retinal rod outer segments on the kinetic parameters of the enzyme. *Biochemical Journal* **265**, 655–658.

Yau, K.-W. & Baylor, D. A. (1989). Cyclic GMP-activated conductance of retinal photoreceptor cells. *Annual Review of Neuroscience* **12**, 289–327.

APPENDIX A

Diffusion of proteins associated with the disc membrane

In this Appendix we present a theoretical consideration of the interactions between the proteins of transduction in the disc membrane as a result of diffusional contact. This analysis is presented in terms of the specific cascade $Rh^* \rightarrow G^* \rightarrow PDE^*$, but it should also be applicable in other comparable cases of diffusional activation mediated by a G-protein.

Enzymatic activation with two-dimensional diffusion, $Rh^* \rightarrow G^*$

We begin by considering the diffusional interaction of a single activated molecule of Rh^* with molecules of G-protein. The molecules need first to collide, and then to react. The diffusion-limited rate of such an enzymatic reaction has been calculated by Naqvi (1974) and Torney & McConnell (1983), through the application to two dimensions of the approaches of Smoluchowski and Noyes. One of the assumptions in this approach is that the reaction between the two diffusing species is equivalent to the case in which the molecule of Rh^* is fixed and the $G \cdot GDP$ diffuses with an effective diffusion coefficient $(D_{Rh} + D_G)$. By 'diffusion-limited' it is meant that the reaction between Rh^* and $G \cdot GDP$ proceeds instantaneously whenever the Rh^* encounters a molecule of $G \cdot GDP$, i.e. the reaction occurs at the collision rate.

The diffusion limit to the rate ν_{RG} at which an Rh^* could activate molecules of G-protein is then given approximately by

$$\nu_{RG} < \frac{4\pi(D_{Rh} + D_G)\,C_G}{\ln\left[4(D_{Rh} + D_G)\,t/\rho^2\right] - 1{\cdot}15}, \tag{A 1}$$

where t is time after the generation of the single molecule of Rh^*, ρ is the encounter distance (the distance apart at which Rh^* and $G \cdot GDP$ interact), and D_{Rh}, D_G and C_G are as defined on p. 724 (see

Table 1). Equation (A1) is a first-order expansion of a more complicated expression, and the approximation is subject to the proviso that the denominator is reasonably large (say > 4; see Naqvi, 1974, p. 282).

In accord with modern views of reactions in two dimensions, eqn (A1) shows that the diffusion-limited reaction rate is not constant, but declines approximately logarithmically with time (Naqvi, 1974; Torney & McConnell, 1983). In the range of times which are of interest to us, however, it turns out that this variation is relatively small, so that ν_{RG} may be approximated as a constant. If we take the effective diameters of rhodopsin and $G_{\alpha\beta\gamma}$ as 2·8 nm and *ca* 7 nm (see Liebman *et al.* 1987) then the encounter distance, given by the sum of the radii, would be approximately $\rho = 5$ nm. With $(D_{Rh} + D_G) = 1\cdot9\ \mu m^2\ s^{-1}$ (see Table 1) we obtain $4(D_{Rh} + D_G)t/\rho^2 = 3\cdot2 \times 10^5\ s^{-1}\ t$. For calculation of the rising phase of the rod photoresponse the times of greatest interest are from about 5–500 ms, i.e. about a log unit either side of $t = 50$ ms. Over this range $4(D_{Rh} + D_G)t/\rho^2$ varies from $1\cdot6 \times 10^3$ to $1\cdot6 \times 10^5$, so that the denominator in eqn (A1) varies from 6·2–10·8, indicating that the limiting value of ν_{RG} varies by about $\pm30\%$ from its limit at $t = 50$ ms.

At $t = 50$ ms the denominator in eqn (A1) equals 8·5, so that eqn (A1) reduces to

$$\nu_{RG} \lesssim 1\cdot5\,(D_{Rh} + D_G)\,C_G. \qquad (A\,2)$$

With $D_{Rh} = 0\cdot7\ \mu m^2\ s^{-1}$, $D_G \approx 1\cdot2\ \mu m^2\ s^{-1}$ (but see p. 757 for qualification), and $C_G \approx 2500\ \mu m^{-2}$, eqn (A2) gives the diffusion-limited reaction rate (or encounter rate) as $\nu_{RG} \lesssim 7000\ s^{-1}$.

In the event that there is any delay other than diffusion which limits the rate of reaction, then the actual rate will be even less dependent on time than is calculated above. Hence, whether or not the reaction is diffusion-limited, it will be appropriate to take ν_{RG} as a constant. Accordingly the average rate $d[G \cdot GTP]/dt$ of activation of G-protein to the form $G \cdot GTP$ may (ignoring inactivation) be taken as

$$d[G \cdot GTP]/dt = Rh^* \nu_{RG}, \qquad (A\,3)$$

where Rh^* represents the number of activated receptor molecules, and where ν_{RG} is a constant. Thus when inactivation reactions are ignored, the quantity of $G \cdot GTP$ will simply rise as the integral of $Rh^*(t)$.

Time course of activation of $G_\alpha^* \cdot GTP$

We need also to allow for any delays in the series of microsteps 2A–2E. (Note that the sum of the delays in Steps 2A–2D cannot exceed ν_{RG}^{-1}.) According to Kahlert & Hofmann (1991), the binding of GTP (Step 2C) may cause a delay, and we shall also allow for the possibility that dissociation of the α-subunit (Step 2E) may not be instantaneous; hence we introduce τ_{2C} and τ_{2E} as the two time constants. The time course of $G_\alpha^* \cdot GTP$ is then found from the delayed integral of $Rh^*(t)$ in eqn (1.2), as

$$G^*(t) = \Phi \nu_{RG}\,\mathrm{ramp}(t) * \mathrm{delay}(\tau_R, \tau_{2C}, \tau_{2E}, t), \qquad (A\,4)$$

where we have employed the terminology ramp(...) and delay(...) defined on p. 723.

Subsequent reaction, $G^* \to PDE^*$

We now consider the subsequent reaction in which the product of the enzymatic step, $G_\alpha^* \cdot GTP$, interacts with the third protein, the PDE. The problem to be analysed is that molecules of $G_\alpha^* \cdot GTP$, which are produced sequentially at various points on the pathway taken by Rh^*, diffuse laterally so as to contact the PDE.

Macroscopic approximation

Since molecules of $G_\alpha^* \cdot GTP$ are expected to be produced at a rate exceeding $1000\ s^{-1}$, it will be appropriate to explore a macroscopic description involving classical diffusion theory. The problem is, however, complicated by the fact that the molecules of $G_\alpha^* \cdot GTP$ are produced not at a single point, but wherever Rh^* happened to be at the time of reaction with a molecule of G-protein; the molecules of $G_\alpha^* \cdot GTP$ then diffuse from these initial locations.

Simplifications

In order to render the problem tractable we shall make several simplifications. Firstly, we shall make the approximation that Rh^* is immobile, so that $G_\alpha^* \cdot GTP$ is produced at a single point, and we shall compensate for this by increasing the effective diffusion coefficient for $G_\alpha^* \cdot GTP$ by an

amount equal to the actual diffusion coefficient D_{Rh} of rhodopsin, in an attempt to allow for the movement that Rh* would already have made. Secondly, we shall make the approximation that the PDE also is immobile, and we shall compensate by further increasing the effective diffusion coefficient of $G_\alpha * \cdot GTP$ by the actual diffusion coefficient D_{PDE} of the PDE. Thirdly, we shall assume that the domain in which the molecules interact is unbounded, i.e. that there are no edge effects and no competition between the reactions of different photons.

Thus the situation we need to analyse is that $G_\alpha * \cdot GTP$, which is produced at a constant rate ν_{RG} (at an arbitrary point defined as $r = 0$), diffuses radially with diffusion coefficient

$$D = D_{Rh} + D_{G\alpha} + D_{PDE}. \tag{A 5}$$

The diffusing $G_\alpha * \cdot GTP$ contacts immobile molecules of PDE, present in the disc membrane at concentration C_{PDE} and each possessing two γ-subunits. The $G_\alpha * \cdot GTP$ reacts with the PDE to produce $PDE_\gamma – G_\alpha * \cdot GTP$ by a mechanism which we shall specify subsequently.

Spatial profile of activated G-protein

With a constant flux at the origin $r = 0$, the solution for the density $g*(r, t)$ of $G_\alpha * \cdot GTP$ has been given by Carslaw & Jaeger (1959), in their eqn §10·4(4), as

$$g*(r, t) = \frac{\nu_{RG}}{4\pi D} E_1 \left(\frac{r^2}{4Dt} \right) \tag{A 6}$$

where $E_1(q)$ is the exponential integral (see Abramowitz & Stegun, 1964, chapter 5). This solution, which is illustrated in Fig. 10, breaks down for very small radii, since we have assumed Rh* to be immobile. A noteworthy feature of the solution is that r and t appear only in the argument of the function, and then in the form $r^2/4Dt$. This has the important consequence that the spatial profile of the solution is invariant with time. Thus, as time progresses, the shape of the solution is unaltered; all that changes is the scaling in the radial dimension, which increases in proportion to $\sqrt{4Dt}$.

Spatial profile of activated PDE

In order to obtain the diffusion limit on the rate of reaction, we shall now assume that $G_\alpha * \cdot GTP$ reacts *instantaneously* with the PDE, according to some saturation function f_{GP}, so that the density $p_\gamma \cdot g_\alpha(r, t)$ of $PDE_\gamma – G_\alpha * \cdot GTP$ is related to the density $g*(r, t)$ of $G_\alpha * \cdot GTP$ by

$$p_\gamma \cdot g_\alpha(r, t) = f_{GP}[g*(r, t)]. \tag{A 7}$$

Hence the density $p_\gamma \cdot g_\alpha(r, t)$ of the reacted form $PDE_\gamma – G_\alpha * \cdot GTP$ is found by application of the saturation relation eqn (A7) to eqn (A6), as indicated by the lowermost curve in Fig. 10. Note that, in this approach, any distortion of the spatial profile of $g*(r, t)$ resulting from the binding of $G_\alpha * \cdot GTP$ to the PDE has been ignored.

Because of the 'radial scaling' property of eqn (A6), the fraction of $G_\alpha * \cdot GTP$ molecules which have reacted to generate $PDE_\gamma - G_\alpha * \cdot GTP$ must be a constant, independent of time. Thus the 'coupling gain' c_{GP}, defined as the ratio

$$c_{GP} = P_\gamma \cdot G_\alpha(t) / G*(t), \tag{A 8}$$

will be a constant; such a situation will apply irrespective of the form of the saturation relation. One way to appreciate this property is to note that the total quantities $P_\gamma \cdot G_\alpha(t)$ and $G*(t)$ represent the integrals (over the whole disc surface) of the functions $p_\gamma \cdot g_\alpha(r, t)$ and $g*(r, t)$ plotted in Fig. 10. Since the abscissa is scaled in proportion to r^2, the factor $P_\gamma \cdot G_\alpha(t)/G*(t)$ is given by the ratio of the areas under the respective curves for $p_\gamma \cdot g_\alpha(r, t)$ and $g*(r, t)$. Hence c_{GP}, the ratio of areas, is a constant for any given saturation function f_{GP} in eqn (A7).

Because this ratio is constant, it follows that the $PDE_\gamma – G_\alpha * \cdot GTP$ will also be produced at a constant rate, so that

$$d[P_\gamma \cdot G_\alpha(t)]/dt = \Phi\nu_{RP}, \tag{A 9}$$

where

$$\nu_{RP} = c_{GP}\nu_{RG}. \tag{A 10}$$

Here ν_{RP} is the rate of production of $PDE_\gamma – G_\alpha * \cdot GTP$ as a result of the presence of a single activated molecule of Rh*.

Limiting case

An important limiting form of the saturation relation f_{GP} applies when $G_\alpha^* \cdot GTP$ reacts with all available γ-subunits of PDE. Because of the existence of two γ-subunits per PDE, the density of activatable subunits will be $2\,C_{PDE}$. In this case the saturation function in eqn (A7) may be written as

$$
\begin{aligned}
f_{GP} &= 2C_{PDE} \quad g^* \geqslant 2C_{PDE} \\
f_{GP} &= g^* \quad\quad\ g^* < 2C_{PDE}
\end{aligned}
\quad, \tag{A 11}
$$

indicated by the continuous curve in Fig. 10. As we have assumed that the reaction between the molecules occurs instantaneously upon every contact, the overall model now corresponds to the *diffusion-limited* activation of PDE subunits by $G_\alpha^* \cdot GTP$.
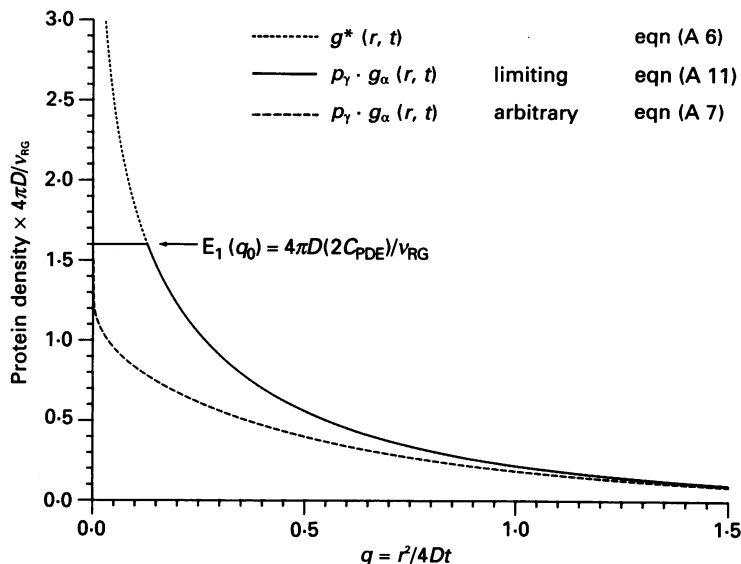
Fig. 10. Spatial profiles of the concentrations (area densities) of the activated forms of the G-protein and the PDE. To allow the exponential integral to be plotted unscaled, the ordinate plots the protein densities scaled by $4\pi D/\nu_{RG}$, and the abscissa plots $r^2/4Dt$ (see eqn (A6)); r is radial distance from the point of isomerization, t is time after the isomerization, and D is the effective lateral diffusion coefficient given in eqn (A5). Since the abscissa is plotted in proportion to r^2, the area beneath each curve gives a measure of the total quantity of the respective form. The uppermost (dotted) curve plots $g^*(r,t)$ as the exponential integral given in eqn (A6); the area beneath this curve represents the total quantity of $G^*(t)$. The lowermost (interrupted) curve plots $p_\gamma \cdot g_\alpha(r,t)$ for an arbitrary binding relation, eqn (A7); the area beneath this curve represents the total quantity of bound $P_\gamma \cdot G_\alpha(t)$. The continuous curve plots the limiting form of binding given in eqn (A11); the area beneath this curve therefore represents the quantity of $P_\gamma \cdot G_\alpha(t)$ in the diffusion limit. The horizontal section of the solid curve represents the original density of PDE subunits, see eqn (A 13).

Substituting eqns (A6) and (A11) into eqn (A7), and integrating $p_\gamma \cdot g_\alpha(r,t)\,2\pi r\,dr$ over all r, we obtain the limiting value of the coupling gain c_{GP} (i.e. the limiting ratio $P_\gamma \cdot G_\alpha / G^*$) as

$$
c_{GP} \leqslant q_0\,E_1(q_0) + E_2(q_0), \tag{A 12}
$$

where the two terms on the right-hand side correspond respectively to the integrals over the two regions specified in eqn (A11), and where q_0 satisfies

$$
E_1(q_0) = 4\pi D(2C_{PDE})/\nu_{RG}. \tag{A 13}
$$

From eqn (5.1.14) of Abramowitz & Stegun (1964), eqn (A12) reduces to the simple form

$$c_{GP} \leqslant \exp(-q_0). \tag{A 14}$$

Substitution of values

From Table 1 we obtain $D = 0.7 + 1.5 + 0.8 \ \mu m^2 \ s^{-1} = 3 \ \mu m^2 \ s^{-1}$, and $C_{PDE} = 167 \ \mu m^{-2}$. If we take the rate of G-protein activation as $\nu_{RG} = 7000 \ s^{-1}$ (see p. 751), then $4\pi D \, 2C_{PDE} / \nu_{RG} = 1.8$, so that eqn (A13) is satisfied by $q_0 \approx 0.112$, and eqn (A14) yields $c_{GP} \leqslant 0.89$. Smaller values of ν_{RG} would result in the limit on c_{GP} being even closer to unity.

Diffusion limit of both reactions

If, in addition to the assumption that activation of the PDE proceeds at the diffusion limit, we make the further assumption that generation of the active G-protein likewise proceeds at the diffusion limit, then it is possible to replace ν_{RG} in eqn (A13) with the expression for its limit from eqn (A2). This leads to the limiting form

$$E_1(q_0) = 4\pi(D_{Rh} + D_{G\alpha} + D_{PDE}) \, 2C_{PDE} / 1.5 \, (D_{Rh} + D_G) \, C_G,$$
$$\approx 26 C_{PDE}/C_G. \tag{A 15}$$

In order that the activation of PDE by the G-protein should not be wasteful, we require c_{GP} to be fairly close to unity. To achieve $c_{GP} \approx 0.9$, for example, eqn (A14) indicates that we require $q_0 < 0.1$, which gives $E_1(q_0) > 1.8$. Substitution of this value in eqn (A15) shows that the requirement will be achieved with $C_{PDE}/C_G > 1.8/26 \approx 1/14$. Thus we can say (more or less independently of membrane fluidity) that a highly 'efficient' activation of PDE can be achieved when the density of PDE molecules is at least 1/14 the density of the G-protein. This is, in fact, very close to the ratio of protein densities found experimentally in the amphibian rod outer segment (Table 1).

Interpretation

In the macroscopic approximation, an inevitable consequence of the ramp-wise generation of $G_\alpha^* \cdot GTP$ is that the production of $PDE_\gamma - G_\alpha^* \cdot GTP$ also ramps with time. In the limit that $G_\alpha^* \cdot GTP$ binds rapidly and tightly to all available γ-subunits of PDE, the coupling gain c_{GP} has an upper limit given by eqn (A14) with eqn (A13). For parameters appropriate to the amphibian rod this limit is close to unity, and we therefore conclude that diffusion *per se* of proteins at the disc membrane will not significantly limit the rate of reaction of $G_\alpha^* \cdot GTP$ with the PDE.

Instead, diffusion at the disc surface will be fast enough so that only a small proportion of $G_\alpha^* \cdot GTP$ molecules remain within a region where their concentration $g^*(r,t)$ exceeds the initial concentration of activatable PDE subunits, $2C_{PDE}$. Hence localized depletion of PDE will not occur to a significant degree with dim flashes, and as a result the rate of reaction will be determined approximately by the Law of Mass Action. Finally, in the case that the activation reactions of both the G-protein and the PDE proceed at their diffusion limits, eqn (A15) shows that a ratio of PDE to G-protein in the disc membrane of roughly 1/14 will be sufficient to ensure that the coupling gain is very high.

First-contact time

In the preceding macroscopic analysis we have implicitly assumed the proteins to be distributed as a continuum. In fact the spacing between molecules is finite, and as a result a small delay in the reaction will be introduced, corresponding to the first-contact time, i.e. the mean time taken for a single $G_\alpha^* \cdot GTP$ to reach the closest molecule of PDE. From the two-dimensional diffusion analysis used to derive eqn (A1), we obtain the first-encounter time τ_{P1} as

$$\tau_{P1} \approx \{3(D_{G\alpha} + D_{PDE}) \, C_{PDE}\}^{-1}, \tag{A 16}$$

analogous to eqn (A2). Substitution of values (see Table 1), gives the first-encounter delay as $\tau_{P1} \approx 0.9$ ms.

Binding according to Law of Mass Action

A second delay stage that needs to be taken into account is introduced because the binding of $G_\alpha^* \cdot GTP$ to the PDE proceeds according to the Law of Mass Action. The formation of the bound state will therefore be delayed from the time course of the increase in concentration of $G_\alpha^* \cdot GTP$

by a pseudo-first-order delay, to which we shall assign a time constant τ_{P2}. Finally, it is possible that subsequent to binding of the $G_x^* \cdot GTP$ a further delay will be involved in the conformational change required for activation of the PDE*, which we shall denote as τ_{P3}. We shall assume τ_{P2} and τ_{P3} to be short.

Time course of activation of PDE*

We can combine the preceding analysis to give the equation for the time course $PDE^*(t)$ of activation of PDE* as

$$PDE^*(t) = \Phi \nu_{RP} \, \text{ramp}(t) * \text{delay}(\tau_R, \tau_{2C}, \tau_{2E}, \tau_{P1}, \tau_{P2}, \tau_{P3}, t), \tag{A 17}$$

where ν_{RP} is given by eqn (A10) with eqns (A14) and (A13), and the term delay(...) is as defined on p. 723.

<center>APPENDIX B</center>

<center>*Solution for the single-photon response*</center>

For the single-photon case, longitudinal diffusion in the cytoplasm must be taken into account, and we need to solve eqn (4.5) which includes the term $\partial^2/\partial x^2$. We shall ignore end effects by assuming the outer segment to be infinitely long; we then redefine the origin $x = 0$ as the point of isomerization, and consider the semi-infinite rod extending in the positive x direction.

Equating the longitudinal flux (obtained from Fick's Law) with the hydrolytic flux at the point of isomerization (from eqn (4.1)) we obtain the boundary condition on eqn (4.5) as

$$\partial cG/\partial x|_{x=0} = PDE_\phi^*(t) \, \beta_{sub} \frac{L}{2D_x} cG(t)_{x=0}, \tag{B 1}$$

where $PDE^*_\phi(t)$ is the time course of PDE activation per isomerization (see eqn (6.5)). Substituting the delayed ramp approximation for $PDE^*_\phi(t)$ from eqn (3.3), the boundary condition becomes

$$\partial cG/\partial x|_{x=0} = \nu_{RP} \beta_{sub} \frac{L}{2D_x} cG(t)_{x=0} \, \text{ramp}(t - t_{eff}). \tag{B 2}$$

This boundary condition is of the 'radiation' type, where the spatial derivative $\partial cG/\partial x$ is expressed in terms of the value of cG at the boundary. To obtain a tractable solution we restrict consideration to sufficiently early times in the response that we may consider $cG(t)_{x=0}$ to be unchanged from its initial value, i.e. we have $cG(t)_{x=0} \approx cG_{dark}$. This means that we restrict consideration to the 'small signal' case, and later we consider the range of times to which this constrains us.

This approximation reduces the boundary condition to the 'flux' type, where the gradient is a defined function of time. For a flux in the form of a ramp at $t = 0$, described by

$$\partial cG/\partial x|_{x=0} = k \, t \, cG_{dark}, \quad t > 0, \tag{B 3}$$

with k a constant, Carslaw & Jaeger (1959) give a solution (§2·9(16)) which reduces to

$$\frac{cG(x,t)}{cG_{dark}} = 1 - k \, 2\sqrt{(D_x t)} \, 4t \, i^3 \text{erfc}(x/2\sqrt{(D_x t)}) \tag{B 4}$$

where $i^m \text{erfc}(u)$ is the repeated integral of the error function.

To obtain the photoresponse we need to substitute this expression into eqn (5.7), taking note of our revised definition of the origin for x as the point of isomerization. Since we are restricted to working with small responses, where $cG/cG_{dark} \approx 1$, we can make use of the approximation that $1 - (1-z)^n \approx nz$ for z small, where the term $(1-z)$ represents the right hand side of eqn (B4). With this approximation, integration of eqn (5.7) (over our two semi-infinite sections of rod) gives the normalised single photon response $R_\phi(t)$ as an expression in terms of $i^4 \text{erfc}(0)$. Noting that $i^{2m} \text{erfc}(0) = 1/(2^{2m} m!)$, we find that the single-photon response $R_\phi(t)$ reduces to

$$R_\phi(t) \approx \frac{n \, k \, D_x \, t^2}{L}. \tag{B 5}$$

Comparison of eqns (B2) and (B3) shows that the constant k may expressed in the form $2kD_x/L = \nu_{RP}\beta_{sub}$. Insertion of these parameters into eqn (B5), with the time origin shifted to t_{eff}, gives the rising phase of the single-photon response as

$$R_\phi(t) \approx \tfrac{1}{2}[\nu_{RP}\beta_{sub}\,n]\,(t-t_{eff})^2, \quad t > t_{eff}. \tag{B 6}$$

From the definition of τ_ϕ in eqn (7.13) this reduces to

$$R_\phi(t) \approx \tfrac{1}{2}\left[\frac{t-t_{eff}}{\tau_\phi}\right]^2, \quad t > t_{eff}. \tag{B 7}$$

It is satisfying to note that eqns (B6) and (B7) in fact represent the same approximation as would be obtained at early times from eqns (6.8) or (6.10), by putting $\Phi = 1$.

Range of validity

The most important restriction in our derivation of the single-photon response above is that it is only valid if the fractional change in concentration of cyclic GMP at the point of isomerization is small, i.e. the simplification in the boundary condition (B3) requires that $cG(t)_{x=0} \approx cG_{dark}$. This simplification places a restriction on the times of validity for the solution, which we now investigate.

Substituting $x = 0$ in eqn (B4) and re-writing the equation in terms of the single-photon response $R_\phi(t)$, it is possible to express the fractional change in concentration of cyclic GMP at the point of isomerization as

$$1 - cG(t)_{x=0}/cG_{dark} \approx R_\phi(t)\left[\frac{L/\sqrt{D_x t}}{1\cdot 33n}\right]. \tag{B 8}$$

Substituting $n = 3$, and values for a toad rod of $L = 60\,\mu m$ and $D_x = 8\,\mu m^2\,s^{-1}$ (see p. 758), we find that the term in square brackets in eqn (B8) equals 7.5 at $t = 500$ ms. Since the normalized single-photon current $R_\phi(t)$ is about 1% at 500 ms in a toad rod (Baylor *et al.* 1979), eqn (B8) indicates that the fractional reduction in cyclic GMP concentration at the origin at that time will be less than 10%; elsewhere it will of course be smaller.

Hence, for at least the first 500 ms in the single-photon response of a toad rod, our assumption that $cG(t)_{x=0}$ is approximately equal to cG_{dark} will be reasonably accurate, and the derivation of eqn (B6) will therefore also be accurate. In salamander rods, which exhibit a shorter length $L = 22\,\mu m$, a very similar diffusion coefficient $D_x \approx 7\,\mu m^2\,s^{-1}$ (Cameron & Pugh, 1990; see p. 64), and a slightly smaller absolute sensitivity at a fixed early time (i.e. slightly longer τ_ϕ), substitution of values shows that the derivation will be accurate for even longer times.

Local saturation

An important corollary of the derivation above is that, during the rising phase of the single-photon response in amphibian rods, the light-sensitive channels are *not* blocked completely over a finite region of the outer segment. Since the fractional reduction in cyclic GMP concentration does not exceed 10% in the first 500 ms of the response, then the fractional closure of channels at the point of isomerization will not exceed 27% at that time, i.e. $1-(1-0\cdot 1)^3 \approx 0\cdot 27$; in a salamander rod the corresponding figure is 10%. Hence, although it is possible that nearly-complete blockage may occur at later times in the single-photon response (for the slow responses of toad rods), it certainly does not occur during the first 500 ms after an isomerization, at room temperature.

Therefore local saturation cannot be used to explain the observed exponential form of the response–intensity relation in these cells at fixed early times (Lamb *et al.* 1981). Instead, we showed in eqn (6.6) that the exponential form may be explained quite simply on the basis of the known cytoplasmic reactions.

APPENDIX C

Estimation of parameters of the amphibian rod outer segment given in Table 1

Protein concentrations

The protein concentrations (area densities) have been determined by Hamm & Bownds (1986) for frog rods; see also Pugh & Lamb (1990) and Kahlert & Hofmann (1991).

Lateral diffusion coefficients of the proteins

Gupta & Williams (1990) have recently measured the lateral diffusion coefficient D_{Rh} for rhodopsin to be $0.73 \ \mu m^2 \ s^{-1}$ in green rods of the toad retina at room temperature, about 80% higher than the value of $ca \ 0.4 \ \mu m^2 \ s^{-1}$ which they and previous workers found in red rods. They speculate that this apparent difference may result not from a difference in diffusion coefficient *per se*, but from the greater number and depth of the incisures in red rods. On this interpretation the larger value would be correct, and so we shall take the lateral diffusion coefficient for rhodopsin in amphibian rods to be approximately $0.7 \ \mu m^2 \ s^{-1}$ at 22 °C.

For the G-protein and the PDE there are no experimental measurements of the diffusion coefficients of which we are aware. However, measurements on peripheral membrane proteins in a variety of preparations (see for example Clegg & Vaz, 1985) suggest that for the holo-G-protein (molecular mass *ca* 80 kDa) the lateral diffusion coefficient would be almost double that of rhodopsin in the same membrane; a similar conclusion has recently been drawn by Kahlert & Hofmann (1991). On this basis, and allowing also for the different molecular weights of the proteins, our estimated lateral diffusion coefficients for $G_{\alpha\beta\gamma}$, G_α and PDE are given in Table 1. These values are, however, only estimates.

Hydrolytic parameters of the PDE

Estimates in the literature for the hydrolytic parameters of the PDE vary widely. In different studies the hydrolytic velocity k_{cat} of the fully-activated PDE* has been reported to range from 800 to 4000 s^{-1}, while the Michaelis constant K_m has been reported to range from 40 μM to 1 mM. The ratio of the parameters, k_{cat}/K_m, varies over a range of more than 100-fold, from 0.5 to 90 $s^{-1} \ \mu M^{-1}$. Hence this approach does not provide a reliable means of estimating β_{sub}, defined in eqn (4.4). Nevertheless, if we take $k_{cat} \approx 2000 \ s^{-1}$ and $K_m \approx 125 \ \mu M$, and if we also take the cytoplasmic volume as $V_{cyto} = 1$ pl and the buffering power for cyclic GMP as $BP \approx 2$ (see below), then eqn (4.4) yields an order-of-magnitude estimate of $\beta_{sub} \approx 6 \times 10^{-6} \ s^{-1}$.

An alternative approach is to divide β_{max}, the estimated maximal value of the rate constant $\beta(t)$, by the estimated total number of PDE subunits in the outer segment, i.e.

$$\beta_{sub} = \beta_{max}/(2 \, PDE_{tot}), \tag{C 1}$$

where PDE_{tot} is the total number of PDE molecules. From the PDE concentration, of $C_{PDE} = 167$ μm^{-2}, we obtain $2 \, PDE_{tot} \approx 5 \times 10^7$ for an amphibian rod outer segment. In ten experiments on voltage-clamped cells exposed to exceedingly bright flashes (not illustrated, but as in Fig. 5), the highest reliable values of $\beta(t)$ had a mean of $168 \pm 35 \ s^{-1}$ (S.D.), and $\beta(t)$ appeared to be asymptoting towards a limit. The suppression of the circulating current is likely to have prevented the observation of the true maximum of $\beta(t)$, and we shall adopt $\beta_{max} = 300 \ s^{-1}$ as a working value. For 5×10^5 total subunits of PDE, this corresponds to $\beta_{sub} = 6 \times 10^{-6} \ s^{-1}$, the same as the rough estimate obtained above by the biochemical approach.

Cytoplasmic buffering power

We shall define the incremental buffering power BP of the cytoplasm for cyclic GMP as

$$BP = dcG_{tot}/dcG \tag{C2}$$

where cG and cG_{tot} are the free and total concentrations of cyclic GMP; BP is equivalent to the parameter η of Hodgkin & Nunn (1988). For a single, rapidly binding buffer, with dissociation constant K_b and total buffer concentration B_{tot}, we obtain

$$BP = 1 + B_{tot} K_b/(cG + K_b)^2. \tag{C 3}$$

Pugh & Lamb (1990) have reviewed the evidence that the PDE possesses two non-catalytic binding sites with K_b values of 160 and 830 nM; with $cG = 4 \ \mu M$, approximately 96 and 83% of these sites will be bound. The PDE membrane density of $C_{PDE} = 167 \ \mu m^{-2}$ is equivalent to a cytoplasmic concentration B_{tot} of 30 μM for each site. Equation (C3) then gives the incremental buffering power as about 2.3, if the binding is rapid. However, there is evidence (see Pugh & Lamb, 1990, p. 1931) that the binding–unbinding reaction is slow for at least one of these sites, so that $BP \approx 2.3$ would be an upper limit. On the other hand, for large changes in cyclic GMP concentration, this

incremental approach leads to an underestimate. For example, when cG drops to one-half (so that the circulating current would have dropped to $F = 1/8$), the incremental buffering power of the PDE roughly doubles to $BP \approx 5$.

Diffusion in the cytoplasm

Lamb *et al.* (1981) analysed the diffusion of cytoplasmic messengers around the stack of discs occupying the outer segment. They showed that radial diffusion is very rapid in comparison with the time course of the light response, and that the longitudinal diffusion coefficient D_x is related to the free aqueous diffusion coefficient D, by

$$D_x = D\,(f_A/f_V)\,/\,BP, \tag{C 4}$$

where f_A is the fraction of the cross-sectional area of the outer segment which is available for longitudinal diffusion, and f_V is the fraction of the total outer segment volume occupied by the cytoplasm. With $D \approx 500\,\mu m^2\,s^{-1}$ for cyclic GMP (comparable to sucrose), $f_A/f_V \approx 1/30$ (see Lamb *et al.* 1981) and $BP \approx 2$, we obtain $D_x \approx 8\,\mu m^2\,s^{-1}$. This theoretical estimate is consistent with the recent experimental estimate of 3–10 (mean 7) $\mu m^2\,s^{-1}$ obtained by Cameron & Pugh (1990).